



OPEN ACCESS

EDITED BY

Narottam Saha,
The University of Queensland, Australia

REVIEWED BY

Daoud Ali,
King Saud University, Saudi Arabia
Marina Cabral Pinto,
University of Aveiro, Portugal

*CORRESPONDENCE

Virendra Kumar Yadav,
✉ yadava94@gmail.com
Timsi Modi,
✉ timsimodi90@gmail.com
Min-Kyu Ji,
✉ mkji@kei.re.kr
Byong-Hun Jeon,
✉ bhjeon@hanyang.ac.kr

RECEIVED 07 February 2023

ACCEPTED 24 May 2023

PUBLISHED 20 July 2023

CITATION

Yadav VK, Modi T, Alyami AY, Gacem A,
Choudhary N, Yadav KK, Inwati GK,
Wanale SG, Abbas M, Ji M-K and
Jeon B-H (2023), Emerging trends in the
recovery of ferrospheres and
plerospheres from coal fly ash waste and
their emerging applications in
environmental cleanup.
Front. Earth Sci. 11:1160448.
doi: 10.3389/feart.2023.1160448

COPYRIGHT

© 2023 Yadav, Modi, Alyami, Gacem,
Choudhary, Yadav, Inwati, Wanale, Abbas,
Ji and Jeon. This is an open-access article
distributed under the terms of the
[Creative Commons Attribution License
\(CC BY\)](https://creativecommons.org/licenses/by/4.0/). The use, distribution or
reproduction in other forums is
permitted, provided the original author(s)
and the copyright owner(s) are credited
and that the original publication in this
journal is cited, in accordance with
accepted academic practice. No use,
distribution or reproduction is permitted
which does not comply with these terms.

Emerging trends in the recovery of ferrospheres and plerospheres from coal fly ash waste and their emerging applications in environmental cleanup

Virendra Kumar Yadav^{1,2*}, Timsi Modi^{3*}, Abeer Yousef Alyami⁴,
Amel Gacem⁵, Nisha Choudhary^{1,3}, Krishna Kumar Yadav^{6,7},
Gajendra Kumar Inwati⁸, Shivraj Gangadhar Wanale⁹,
Mohamed Abbas¹⁰, Min-Kyu Ji^{11*} and Byong-Hun Jeon^{12*}

¹Department of Biosciences, School of Liberal Arts and Sciences, Mody University of Science and Technology, Sikar, Rajasthan, India, ²Department of Life Sciences, Hemchandracharya North Gujarat University, Patan, Gujarat, India, ³Department of Environment Sciences, School of Sciences, P P Savani University, Surat, Gujarat, India, ⁴Department of Chemistry, College of Science and Arts, Najran University, Najran, Saudi Arabia, ⁵Department of Physics, Faculty of Sciences, University 20 Août 1955, Skikda, Algeria, ⁶Faculty of Science and Technology, Madhyanchal Professional University, Bhopal, India, ⁷Environmental and Atmospheric Sciences Research Group, Scientific Research Center, Al-Ayen University, Thi-Qar, Nasiriyah, Iraq, ⁸Department of Chemistry, Medicaps University, Indore, Madhya Pradesh, India, ⁹School of Chemical Sciences, Swami Ramanand Teerth Marathwada University, Nanded, Maharashtra, India, ¹⁰Electrical Engineering Department, College of Engineering, King Khalid University, Abha, Saudi Arabia, ¹¹Korea Environment Institute, Sejong, Republic of Korea, ¹²Department of Earth Resources and Environmental Engineering, Hanyang University, Seoul, Republic of Korea

Coal fly ash (CFA) is a major global problem due to its production in huge volumes. Fly ash has numerous toxic heavy metals; thus, it is considered a hazardous material. However, it also has several value-added minerals like ferrous, alumina, and silica along with other minerals. Fly ash also has several natural micro- to nano-structured materials; for instance, spherical ferrous-rich particles, cenospheres, plerospheres, carbon nanomaterials, and unburned soot. These micron- to nano-sized particles are formed from the molten slag of coal, followed by condensation. Among these particles, plerospheres which are hollow spherical particles, and ferrospheres which are ferrous-rich particles, have potential applications in the environmental cleanup, research, catalytic industries, and glass and ceramics industries. Additionally, these particles could be further surface-functionalized or purified for other applications. Moreover, these particles are widely explored for their potential in the army and other defense systems like lightweight materials and sensing. The recovery of such particles from waste fly ash will make the process and remediation technology economically and environmentally friendly. The current review focuses on the various structural and elemental properties of ferrospheres and plerospheres from fly ash. This review also focuses on the emerging applications of both naturally formed materials in CFA.

KEYWORDS

coal fly ash, plerospheres, cenospheres, ferrospheres, ceramics

1 Introduction

Coal fly ash (CFA) is a fine spherical powder produced in thermal power plants (TPPs) during the burning of pulverized coal when generating electricity (Yadav and Fulekar, 2020) (Yadav et al., 2023a). Annually, a large amount of CFA is produced globally and is mainly dumped in the vicinity of thermal power plants (TPPs) (Yadav et al., 2022a). However, due to the rapid advancement in technology, CFA has gained importance in the fields of metallurgy, ceramics (dos Santos et al., 2014), civil applications (Marinina et al., 2021), building and construction (Mohammed et al., 2021), river and embankments, and agriculture (Yadav and Pandita, 2019). The utilization of CFA worldwide is gradually increasing annually. As per a 2022 report, the total global annual production was about 1.143 billion tons, with an average utilization rate of 60%. Several European and Asian countries, including China, also reached 100% CFA utilization rates, while developing countries like India are struggling with a 50%–60% utilization rate as per 2021–2022 data (Yadav et al., 2022a).

The source of CFA is coal, which has various organic and inorganic compounds that produce structurally diverse spherical particles upon burning in TPP furnaces (Yadav et al., 2021a). The structural diversity in CFA particles is due to combustion at high temperatures (1,400–1800°C) (Wang et al., 2021), which melts the content of the coal. Condensation and complex processes give rise to structurally and chemically diverse spherical particles (“spheres”). Such spherical particles could be rich in alumina and silica and are known as “aluminosilicate spheres” or “cenospheres” (Yadav et al., 2021b). Another spherical particle in CFA is “plerospheres,” or spheres within spheres; i.e., larger spheres encapsulating several smaller spheres along with gases and mineral fragments (Chepaitis et al., 2011). Another type of sphere present in CFA is ferrospheres, which are ferrous-rich spherical particles. The size of all these spherical particles varies from 80 nm to several microns (20 μ) depending on the operating conditions of the TPPs (Yadav et al., 2022b). These spherical particles have applications in ceramics, construction, research, and environmental clean-up (Sharonova et al., 2015) and can be separated from CFA by several techniques, most commonly magnetic separation (Shoumkova, 2011; Gupta et al., 2022). For instance, magnetic fractions in CFA could be recovered by using an external magnet in wet or dry magnetic separation methods, while the rich non-ferrous fractions in plerospheres and cenospheres could be extracted using the sink-float technique, froth floatation technique, density-based separation, etc. Cenospheres are lighter in weight in comparison to ferrospheres and plerospheres (Noor-ul-Amin, 2014).

Generally, CFA has mainly 5%–15% ferrous fractions, while plerosphere content varies from 0.1 to 3.8 wt.%. In most cases, it is near 0.3–1.5 wt.%. In the last decade, ferrospheres have been used widely in ceramics, research, and other industries in comparison to plerospheres due to their easy recovery, wider applications in catalysis, etc. Contrary to ferrospheres, very limited information is available on plerospheres (Anshits et al., 2021). These structurally varied spherical particles have different structural and elemental properties and have started gaining importance in various applications (Goodarzi and Sanei, 2009). Several investigators

have reported the recovery of CFA components like cenospheres, plerospheres, ferrospheres, and unburned carbon particles. For instance, Blissett and Rowson (2012) suggested the utilization of CFA for agriculture, zeolite synthesis, cement manufacturing, glass ceramics, geopolymers, etc. (Blissett and Rowson, 2012). Yao and colleagues demonstrated the importance of CFA in the synthesis of geopolymers, silica aerogels, carbon nanotubes (CNTs), etc. (Gollakota et al., 2019). Furthermore, Yao and team emphasized the recovery of alumina from CFA in China (Yao et al., 2014; Gollakota et al., 2019).

The present study mainly emphasized ferrospheres and plerospheres, due to their morphological and elemental properties that make them two distinct, naturally formed spherical ceramic particles in CFA in TPPs. We also described the detailed mechanism involved in the formation of both these spherical particles in the furnace during coal burning in TPPs. Another objective was to summarize the recent advances in the recovery of plerospheres and ferrospheres from CFA. The final objective was to emphasize the emerging applications of plerospheres and ferrospheres in the fields of environmental cleanup and military. More recent work in these fields will draw the attention of scientific investigators toward plerosphere recovery and new emerging applications.

2 Structurally important and value-added particles in CFA

The structurally different structures of CFA i.e., plerospheres (PS), ferrospheres (FS), cenospheres (CS), and irregular carbonaceous particles (Snellings et al., 2021), play specific roles in different fields like environmental cleanup, research, ceramics (dos Santos et al., 2014), fillers, and lightweight materials (Balapour et al., 2022), etc. Among microspheres in CFA, cenospheres are the most predominant, followed by ferrospheres and plerospheres (Liu et al., 2018). All these three microspheres constitute a specific fraction of the CFA that forms as a result of the burning of pulverized coal in the furnaces of TPPs. These microspheres are formed during combustion in the furnace at the stage of transformation of coal mineral compounds, as shown in Figure 1. The spherical shape is attributed to the cooling and solidification of CFA particles around the gases. These microspheres are mainly made up of aluminosilicate glasses, mullite, calcium silicates, sulfate, calcite ferrous oxides, and quartz (Baziak et al., 2021).

Silica dominates the solid phase of these microspheres, whose percentage is about 50%–65%, followed by alumina at 19%–65% and Fe₂O₃ at 0.7%–6.5%. In addition to this, it also has unburned carbons (UC) which are mainly composed of inorganic and organic carbon materials formed from the incomplete combustion of coal (Eisele and Kawatra, 2002; Song et al., 2021; Lv et al., 2022). These unburned particles contain char soot, polyaromatic hydrocarbons, and carbon nanotubes (CNTs) (Alam et al., 2021). Based on various reports around the globe, it was found that the UC content in CFA could vary from 2% to 12% but in some cases could also reach 20% (Liu et al., 2014). There are several reports where both single and multi-walled CNTs were found and isolated from CFA. In addition to this, a few

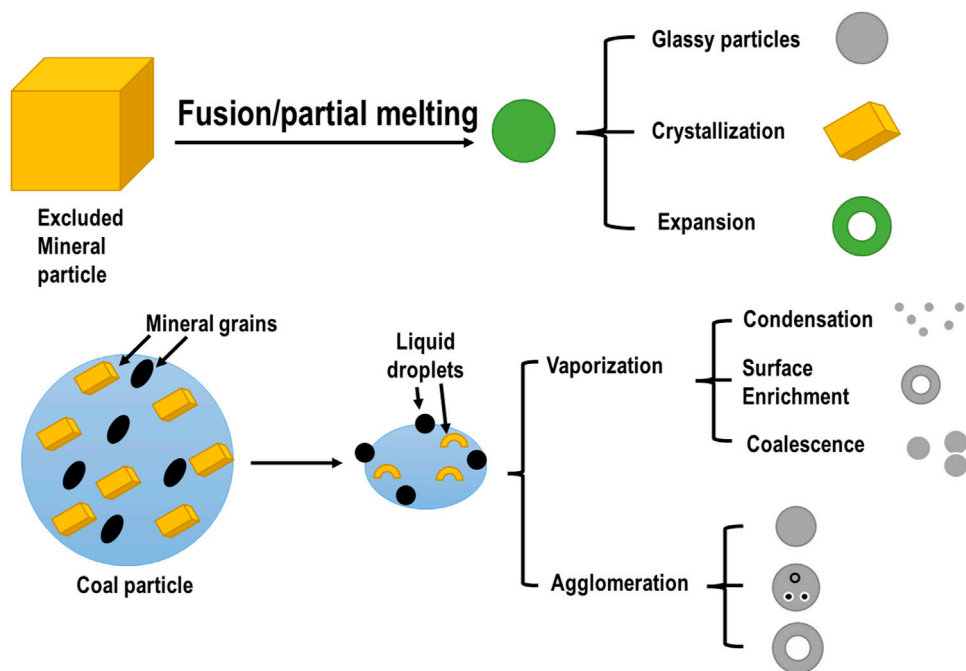


FIGURE 1
Generalized scheme of the transformation of coal mineral matter during combustion. Adapted and modified from [Kutchko and Kim \(2006\)](#).

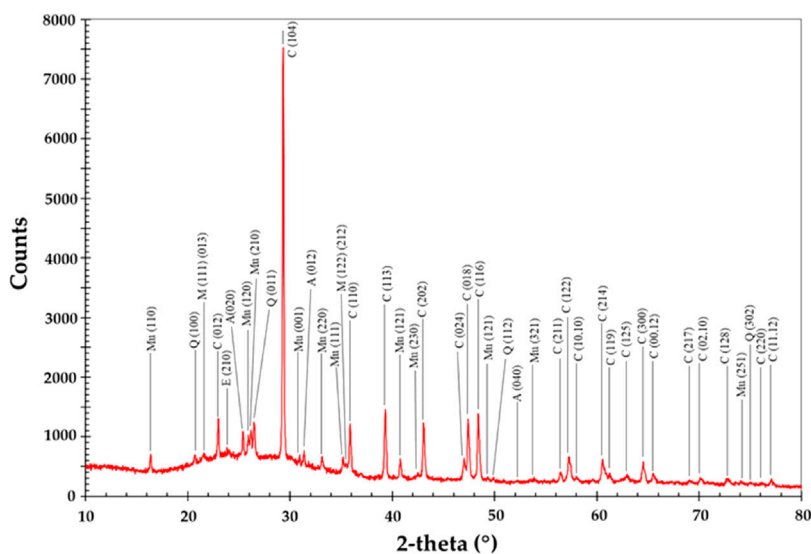


FIGURE 2
XRD of CS from lignite CFA of a Thailand TPP depicting their major minerals. Adapted from [Yoriya and Tepsri \(2020\)](#) and [\(Yoriya and Tepsri, 2021\)](#).

investigators have also reported the extraction of fullerene, nanoions, and graphene from CFA ([Das et al., 2016](#); [Liu et al., 2016](#); [Gnanamoorthy et al., 2021](#)). [Tiwari et al. \(2016\)](#) reported the presence of fullerene-like aggregates in CFA ([Tiwari et al., 2015](#)). The presence of CNTs 18–24 nm in diameter in the Gondwana region CFA was reported by a group of investigators from India.

Several investigators have also claimed the presence of carbon nanoballs in various CFAs from different parts of the globe, for instance, carbon nanoballs with sizes of 5–10 nm were reported. In addition to these, numerous investigators have reported the presence and recovery of carbon onions, chars, and soots from the CFA samples using various techniques, with very high efficiency.

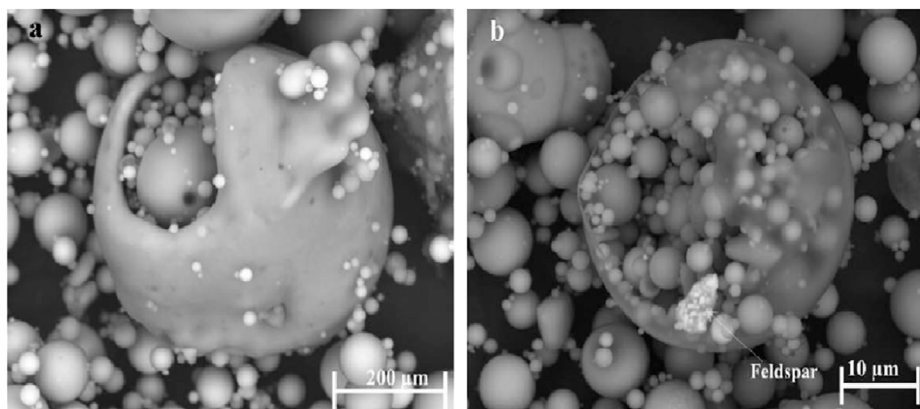


FIGURE 3

(A) SEM image of a thick-walled PS with a ruptured wall. (B) SEM image of a thin-walled PS with a ruptured wall. Adapted from [Goodarzi and Sanei \(2009\)](#).

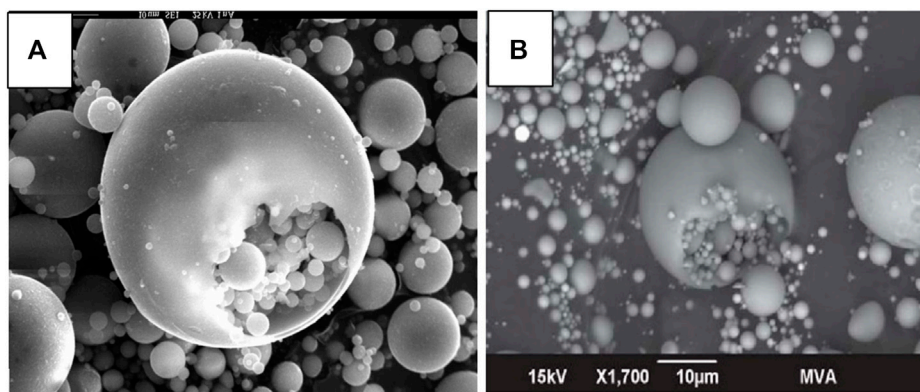


FIGURE 4

(A) SEM micrograph of glassy PS in CFA. Adapted from [Kaasik et al. \(2005\)](#). (B) Backscattered SEM image of PS. Adapted from [Chepaitis et al. \(2011\)](#).

In addition to this, there are several reports where CS were used either directly or surface functionalized with other metallic particles like Ni, Zr, etc., for enhanced applications. CS have been used for the direct remediation of dyes and other effluents from wastewater at a much more economical cost ([Markandeya et al., 2021](#)). In addition to this, surface-functionalized CS are also used in defense applications, nanocomposites, and high mechanical strength material. CS were also used in construction materials, as a lightweight material, an insulating material, in ceramics, as fillers, as a composite material, and as an internal curing agent ([Birla et al., 2017](#); [Yadav et al., 2021b](#)). [Vereshchagina et al. \(2018\)](#) synthesized analcime zeolite from CFA CS, and furthermore, they developed a Zr-analcime nanocomposite from CFA CS ([Vereshchagina et al., 2018](#)). [Khoshnoud and Abu-Zahra \(2015\)](#) observed the effect of CS CFA on the thermal, mechanical, and morphology of rigid polyvinyl chloride (PVC) composites ([Khoshnoud and Abu-Zahra, 2015](#)). [Figure 2](#) shows an XRD pattern of CS from lignite CFA from Thailand TPPs, which clearly shows minerals like anhydrite,

C—calcite, CS—calcium silicate, E—ettringite, L—lime, M—magnetite, Me—merwinite, Mu—mullite, P—potassium magnesium silicate, Po—portlandite, Q—quartz, and Sr—srebrodolskite ([Yoriya and Tepsri 2021](#)).

3 Basic properties of plerospheres and ferrospheres

3.1 Plerospheres

Morphologically, PS are similar to CS and co-exist in CFA in mainly two types, i.e., thick-walled and thin-walled. PS could also be categorized into primary plerospheres and secondary plerospheres (based on internal particles and composition). PS contain several smaller spherical particles within them, making them heavier ([Kolay and Singh, 2001](#); [Sunjidmaa et al., 2019](#)). As per the literature, the ruptured PS contain Fe, which is produced from the disoxidation of

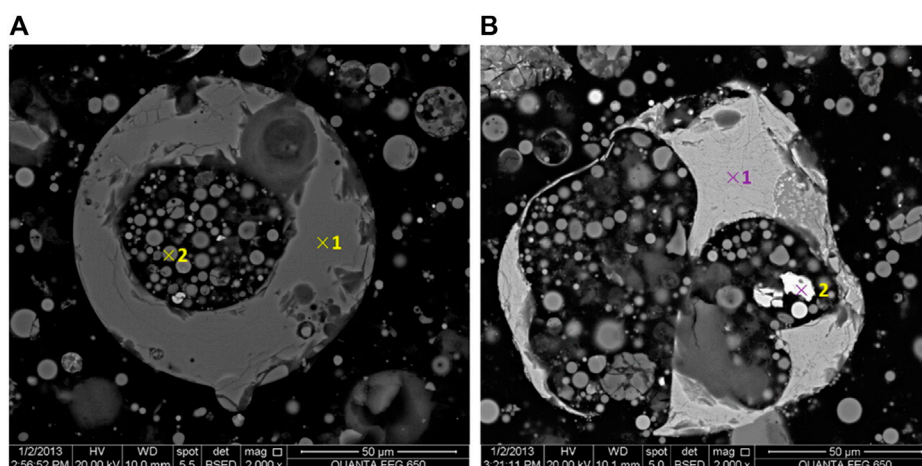


FIGURE 5

(A) Typical SEM image of a plerosphere. (B) SEM image of a cracked PS filled with metallic Fe. Adapted from Liu et al. (2016).

TABLE 1 Chemical composition of CS classified according to their sizes. Adapted from Yoriya and Tepsri (2021).

Item	Composition (wt. %)							
	SiO ₂	Al ₂ O ₃	Fe ₂ O ₃	CaO	SO ₃	K ₂ O	TiO ₂	MnO
Cenospheres								
Bulk	47.23 ± 0.56	22.92 ± 0.14	9.71 ± 0.48	10.89 ± 0.27	3.98 ± 0.12	4.54 ± 0.15	0.80 ± 0.02	0.06 ± 0.00
<45 μ	41.31 ± 0.16	19.61 ± 0.21	12.62 ± 0.15	15.50 ± 0.13	6.47 ± 0.10	3.76 ± 0.02	0.63 ± 0.00	0.11 ± 0.005
45–105 μ	53.39 ± 0.17	25.02 ± 0.06	7.84 ± 0.06	6.36 ± 0.11	1.88 ± 0.11	4.72 ± 0.07	0.78 ± 0.02	0.06 ± 0.001
106–250 μ	51.92 ± 0.23	23.72 ± 0.13	9.70 ± 0.11	8.28 ± 0.21	1.99 ± 0.04	3.57 ± 0.04	0.77 ± 0.005	0.06 ± 0.003
>250 μ	49.71 ± 0.93	20.80 ± 0.59	11.62 ± 0.99	11.56 ± 0.29	2.28 ± 0.31	3.23 ± 0.15	0.72 ± 0.02	0.08 ± 0.001

Fe²⁺ or Fe³⁺ in a strongly reducing environment before the rupture of PS (Adesina, 2020). Plerospheres are basically spheres within spheres, where smaller spherical particles become trapped inside larger spherical particles along with numerous minerals and gases. As a result, such plerospheres may be hollow and light in comparison to ferrospheres (Goodarzi and Sanei, 2009). These PS are mainly thin-walled compared to FS. The sizes of PS vary from a few microns (μ) to more than 20 μ; however, their average size is mainly <10 μ (Liu et al., 2016). Plerospheres (Goodarzi and Sanei, 2009) (or spheres within spheres) are essentially spherical-shaped, hollow, and mostly thin-walled CFA particles that have encapsulated a number of sub-microspheres or mineral particles (Goodarzi and Sanei, 2009) of different sizes (mainly <10 μ) (Liu et al., 2016). Most of their features, such as chemical and elemental composition, morphology, etc., are similar to cenospheres. However, the two vary in their morphology as cenospheres are hollow in nature, while plerospheres are solid in nature (Choudhary et al., 2020). It has been found that in some CFA samples, CS were larger, while in others, PS were larger. However, normally, PS should be larger due to the presence of filled gases and minerals. The size of PS varies from 0.2 to 8 μ, while the size of CS is 10–1,000 μ based on the TPPs, combustion temperature, and types of coal used (Yoriya et al.,

2019; Yoriya and Tepsri, 2020). Ruptured PS release numerous smaller microspheres and mineral particles (Strzałkowska, 2021), as shown in Figures 3A, B, 4A, B, 5A, B where scanning electron microscope (SEM) images show ruptured PS with numerous small spherical particles present within them. To date, very little information is available on PS in the scientific community.

Structurally, PS is either thick- or thin-walled. Based on their origin and formation, they could be of two types, primary plerospheres and secondary plerospheres (Goodarzi and Sanei, 2009). These structurally different types of PS form due to high-temperature (1,200–1,700°C) thermochemical transformation of the organic matter and mineral components in coal during combustion (Liu et al., 2016). PS form due to the differential melting of particles and the influence of gases generated by the: 1) dehydration of clay minerals and 2) decomposition of calcium carbonate and carbon present on the surface or inside the ash slag particles (Fisher et al., 1976). This type of method of PS formation is known as a primary process. PS with larger diameters (e.g., 100 μ) are very common in CFA, enclosing sub-microspheres or mineral fragments (mostly <10 μ) and reportedly have high mechanical strength and chemical reactivity (Snellings et al., 2021).

TABLE 2 Chemical composition of CFA PS. Adapted from [Haustein and Kuryłowicz-Cudowska \(2020\)](#) and [Chepaitis et al. \(2011\)](#).

Element	CFA plerosphere wt. %
Si	25.54
Al	10.93
Mg	0.99
Na	2.92
Fe	—
Ca	1.17
P	—
S	—
K	4.03
Ti	—
C	10.39
O	44.03

PS have generally spherical-shaped particles with several smaller particles and mineral fragments ([Yoriya and Tepsri, 2020](#)). Both thick- and thin-walled PS release secondary plerospheres or mineral particles after wall rupture. As the name suggests, thick-walled plerospheres have thick walls due to a coating of carbon and other minerals. [Figure 5A](#) shows a typical structure of PS under SEM, while [Figure 5B](#) shows PS with ferrous content ([Liu et al., 2016](#)). Very little research has been conducted in this area, and limited information is available in the scientific domain. [Table 1](#) shows the chemical composition of fly ash CS, which indicates that CS are rich in Al and Si. From the chemical composition, one can easily conclude that both CS and PS contain mainly alumina and silica, along with other intermediate and trace elements such as Na, Mg, Ca, K, P, S, and Ti. The carbon composition could be higher or lower based on the type of coal used for the fuel in the TPPs, and other operating conditions of the furnaces of the TPPs. [Yoriya and Tepsri \(2020\)](#) reported that the chemical composition of CS depended on the size of the particles, even though their basic elements remained the same. The CS size and chemical composition were assessed in CS collected from lignite CFA from Thailand TPPs. [Table 2](#) shows the chemical compositions of PS extracted from CFA. [Table 3](#) shows the major differences and similarities between FS, CS, and PS extracted from CFA.

[Figures 6A, B](#) show the energy-dispersive spectroscopy (EDS) spectra and elemental composition of PS and CS, respectively. [Figures 6A, B](#) show the presence of common elements in both structures. The EDS shows that both structures vary only in the percentage of elements. The major elements are Al, Si, O, and Fe. Other elements are present in trace amounts in both structures.

3.2 Ferrosphere properties and types

FS are present in all CFAs, i.e., they are produced from lignite, bituminous, sub-bituminous, and anthracite. They are known as

magnetic microspheres or spinels. A typical FESEM image of FS is shown in [Figure 7](#), which reveals the presence of several spherules and angular deposits of iron oxides on their surfaces.

The major mineralogical composition of magnetic fractions of CFA are ferrosinels (79%–90% wt.%). The FS of CFA have all three phases of iron oxides, i.e., magnetite along with Ca, Mg, and Mn, with hematite comprising approximately 5–17 wt. %, maghemite $\gamma\text{-Fe}_2\text{O}_3$, and a paramagnetic phase of approximately 2–8 wt% ([Sokol et al., 2002](#); [Sokolar and Vodova, 2011](#)). FS are ferrous-rich spherical particles that can be rough or smooth based on the deposition of the ferrous fraction on the surface of aluminosilicate spheres ([Yadav et al., 2021a](#)). These can be of various shapes and sizes, depending on their surface texture, the type of coal used, the temperature of the furnace, etc. CFA-extracted FS morphology can be either rough or smooth, in which the rough spheres show depositions of ferrous particles on their surface and are comparatively more magnetic than the smooth-surfaced ones ([Sokol et al., 2002](#); [Sokolar and Vodova, 2011](#)). The two most dominant types of FS in CFA are rough- and smooth-surfaced FS. These iron-rich microspheres are formed during the combustion of coal, followed by the melting and condensation of the liquid mixes in the TPPs. Rough-surfaced FS have several ferrous-rich granular depositions on their surface, whereas the smooth-surfaced ferrospheres have a homogenous spread of molten ferrous on the surface, which is responsible for the weakly magnetic nature of the particles ([Fomenko et al., 2021](#)). Vast works of literature have shown that, based on the various operating conditions and global area, the size of FS varies from 90 nm to 20 μ ([Liu et al., 2016](#)). Fine CFA contains smaller-sized particles, while bottom CFA contains larger-sized CFA particles along with FS.

Several investigators have isolated ferrous fractions from CFA from various parts of the globe. For instance, [Yadav and Fulekar \(2014\)](#) reported the extraction of ferrous fractions from CFA collected from TPPs in Gandhinagar, Gujarat, India ([Yadav and Fulekar, 2014](#)). [Yadav 2019](#) reported the presence of smooth and rough-shaped ferrous fractions in the CFA of the same TPPs. In both reports, the investigators observed FS sizes varying from 100 nm to several microns. The iron oxides on their surface were mainly present in mixed phases, i.e., magnetite, hematite, and maghemite, as revealed by x-ray diffraction (XRD). Moreover, [Yadav et al. \(2022a\)](#) extracted FS from CFA collected from TPPs in Kota, Rajasthan. The investigators extracted the FS from the CFA slurry using a strong magnet. Most of the FS were rough-surfaced, with angular and spherule depositions on their surface. The size of the extracted FS varied from 400 to 700 nm ([Yadav et al., 2022b](#)).

[Sharonova et al. \(2015\)](#) reported the extraction of approximately eight fractions of FS from high calcium-containing CFA collected from a Russian TPP. The size of the extracted FS varied from 0.4 to 0.02 mm ([Sharonova et al., 2015](#)). [Valentim et al. \(2016\)](#) extracted FS from CFA collected from TPPs in Bokaro and Jharia. The investigators reported that the coal used to feed the TPPs mainly contained ferrous carbonates like siderite. Whereas in the CFA, the iron oxide content was about 2.7 wt.% to 4.5 wt.%. The investigators also confirmed the presence of magnetite and hematite phases of iron oxides in minor ratios in the CFA ([Valentim et al., 2016](#)). [Fomenko et al. \(2021\)](#) extracted ferrous fractions and categorized them according to size, i.e., particulate matter (PM_{2.5}, PM_{2.5–10}, and PM₁₀) ([Fomenko et al., 2021](#)). [Sokol et al. \(1998\)](#) extracted FS

TABLE 3 Basic differences and similarities between FS, PS, and CS extracted from CFA.

Property/feature	Ferrospheres	Plerospheres	Cenospheres	Reference
Shape and types	Spherical, ellipsoidal, molten drop, etc.	Spherical, and thick- and thin-walled	Spherical	
Size (μ)	1–500 μ	0.2–8 μ	10–1000 μ 20–300 μ	Żyrkowski et al. (2016) , Yoriya and Tepsri (2021)
Definition/meaning	—	Plerosphere from Greek: plērēs + sphere = filled sphere	Cenosphere is derived from Greek: kenos + sphere = hollow sphere	
Shell thickness (μ)	—	—	2–30 μ	
External texture	Rough to smooth	Smooth, some with an opening at one end	Smooth	
Internal structure	Solid	Solid Partially filled with porous magnetite-hematite aggregates	Hollow Can have very thin (tenuisphere) or thick walls (crassisphere)	Zierold and Odoh (2020)
Voids filled with	—	Small irregular aluminosilicate grains, unburnt (fusained) coal particles, foam, and spongy and porous framework	Irregular aluminosilicate grains (mainly mullite), iron oxides, unburnt (fusained) coal particles, and spongy (porous) form	
Magnetic nature	Highly magnetic	Non-magnetic to weakly magnetic	May be weakly magnetic	Yoriya and Tepsri (2021)
Percentage in CFA wt. %	5%–15%	0.1–3.8 wt.%	0.3%–1.5%	Fomenko et al. (2011)
Density	2.4 higher density than PS and CS	Higher than CS 0.75–9.0 wt.% Due to its high density, more easily captured by an electrostatic precipitator	Low density for lighter CS: 0.2–2.6 g/cc For heavy metal and Al-bearing CS-02.9 g/cc Average density <1 g/cm ³	Żyrkowski et al. (2016)
Mechanical strength	High	High	Very high	Żyrkowski et al. (2016)
Porosity	Lowest	Highly porous Due to high porosity, most PS sink in water with CFA	Less porous	
Specific gravity	—	Higher	Lowest	Yoon and Park (2017)
Crystalline phases	Magnetite, hematite, quartz, calcite, etc.		Quartz, mullite, calcite Higher alumina and higher mechanical strength	Żyrkowski et al. (2016)
Chemical composition	Fe, O, and traces of Al, Si, Ca, Na, C, etc.	Dominated by Si, Al, C, O, and traces of Fe, Ca, Na, etc.	Dominated by Si, Al, C, O, and traces of Fe, Ca, Na, etc.	Fisher et al. (1976)
Separation method	Magnetic and density-based, and easy to separate	Non-magnetic and density-based	Non-magnetic and density-based	Fomenko et al. (2021)
Applications	Ceramics, petroleum cracking, adsorbents, research, and medicine	Ceramics	Ceramics, defense, and nanocomposites	Liu et al. (2014) Guedes and Valentim (2021) Kanhar et al. (2020)

from the Russian Chelyabinsk basin and reported the presence of magnetic particles of variable geometrical shape; i.e., triangular, rectangular, spherule, and polygonal on the external surface of the FS. They also reported the presence of dense dendritic FS about 50–120 μ in size, which comprised about 85% wt. fraction of the total ferrospheres. Furthermore, investigators also reported the

presence of magnetic particles on FS in a “pine-tree” pattern and ferrite FS with dimensions in the range of 100–200 μ , which was rare in occurrence and comparatively larger than other FS. Finally, the investigators found magnesioferrite in the CFA, which had high reflectivity and formed octahedra 10 μ in size in the microsphere core, whose spaces were filled with calcium ferrite ([Sokol et al., 2002](#)).

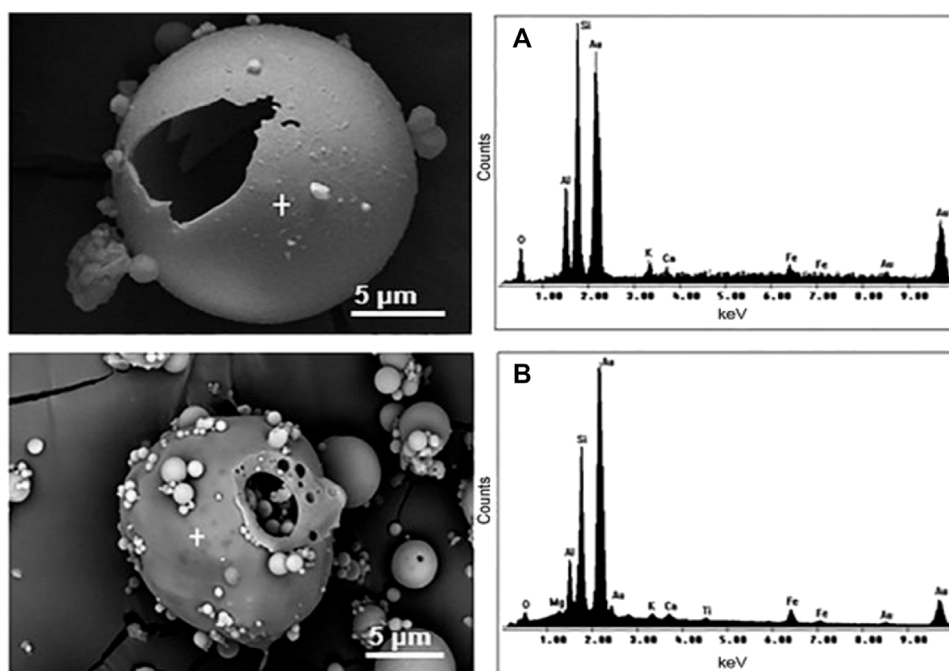


FIGURE 6
SEM micrographs and EDS spectra of CS (A) and PS (B). Adapted from Ferrarini et al. (2016).

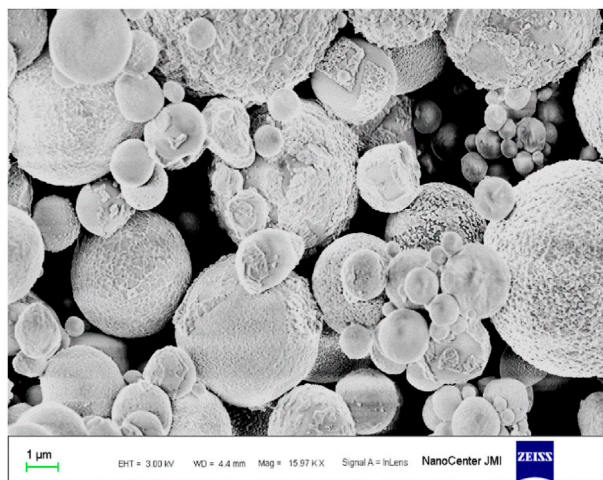


FIGURE 7
FESEM micrographs of CFA ferrospheres. Adapted from Yadav et al. (2020a).

Rough-surfaced ferrospheres have depositions of ferrous particles on their surfaces and are comparatively more magnetic than the smooth-surfaced ferrospheres (Sokol et al., 2002; Um and Jeon, 2021). Rough-surfaced ferrospheres have several ferrous-rich granular depositions on their surface, while smooth-surfaced ferrospheres have a homogenous spread of molten ferrous on their surfaces, which is responsible for their weakly magnetic nature (Fomenko et al., 2021). It is evident from the literature

that the iron oxides in the ferrospheres of CFA are present in all three phases; i.e., magnetite, maghemite, and hematite on the surface of ferrospheres, mainly in the magnetite (Fe_3O_4) and hematite ($\alpha\text{-Fe}_2\text{O}_3$) phases. Several investigators have confirmed the presence of hematite and magnetite (Xue and Lu, 2008; Valentim et al., 2016; Anshits et al., 2018; Yadav et al., 2022b) in CFA collected from different parts of the globe.

All these ferrous granules are deposited on the spheres where the ferrous particles are deposited in the form of dendrites. The ferrous particles/granules are deposited on the ferrospheres during the vaporization and condensation of CFA particles (Sokol et al., 2002). From the literature, it is also well-proven that the source of such ferrous particles is coal, which contains pyrite minerals. At high temperatures in the furnaces of TPPs, these pyrite minerals undergo oxidation and reduction and are transformed into iron oxides. From the literature, the ferrous content of CFA mainly varies from 5% to 15%. This range could vary marginally, based on the area of the globe. Numerous investigators have tried to isolate the ferrous fractions from the CFA, either by dry magnetic or wet slurry-based magnetic separation techniques. The dry magnetic separation technique involves the use of conveyor belts with magnetic fittings at one side to collect the magnetic fractions of the CFA. The slurry-based wet magnetic separation method involves the use of liquid for mixing the CFA. This is followed by a collection of magnetic fractions using a strong magnetic or applied magnetic field (Xue and Lu, 2008).

Regarding the elemental composition, CFA mainly comprises Si, Al, Ca, Fe, and O and traces of Na, K, P, Ti, etc. Ferrospheres are rich in Fe and mainly present with Al, Si, Ca, Ti, and O. The matrix is made up of Al and Si, while the surface contains ferrous. The

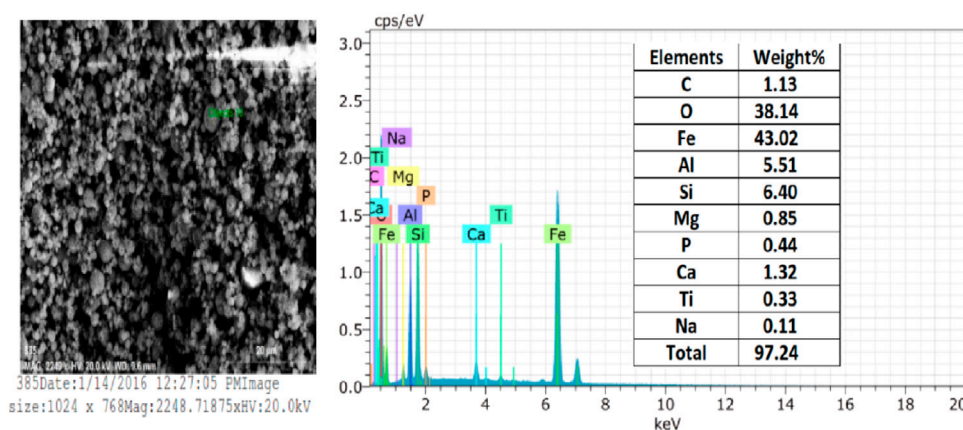


FIGURE 8
EDS spot, EDS spectra, and elemental composition of ferrospheres. Adapted from [Yadav et al. \(2022b\)](#).

composition of such ferrospheres may slightly vary due to the source of coal used in the TPPs, which may be a rich source of other minerals depending on the mines. EDS analysis in the literature revealed appreciable amounts of Si, S, Al, and Ca in ferrospheres, which may come from quartz, mullite ([Yadav et al., 2020b](#)), anhydrite, and amorphous materials in the CFA. Therefore, the major elemental compositions of ferrospheres are Fe and O along with Ca, Mg, Na, K, Ti, and C. The presence of Al, Si, C, Ti, Ca, Mg, etc., along with Fe in extracted FS has been reported by several investigators ([Xue and Lu 2008](#); [Valentim et al., 2016](#); [Sokol et al., Anshits et al., 2018](#); [Yadav et al., 2022b](#)) in CFA collected from different parts of the world. [Yadav et al. \(2022a\)](#) reported the presence of approximately nine elements in their oxides in CFA collected from the Kota TPPs by EDS analysis, as shown in [Figure 8](#). Here, Fe was present in the highest percentage (43.02%) followed by elemental Si (6.4%) and Al (5.51%). O was present at about 38.14%. The CFA also contained traces of Na, Ti, Ca, P, Mg, and C.

Extracted FS have several elemental impurities in the form of Al, Si, Ca, C, etc. so are widely used in the petroleum industries as a catalyst, as well as cokes in the steel industry, etc. However, hardly any literature is available in which these CFA ferrospheres have been used in highly pure form in research or industries. Attempts have made to utilize these ferrous fractions from CFA as a source of raw material for the synthesis of iron particles. In one recent attempt, [Yadav \(2019\)](#) synthesized highly pure iron oxide nanoparticles from CFA by treating the extracted FS with strong mineral acids. Here, the extracted FS was treated with strong acids to obtain ferrous leachate, which in turn was used as a precursor material for the synthesis of IONPs by chemical coprecipitation ([Yadav, 2019](#)).

3.3 Types of ferrospheres

Structurally, FS extracted from CFA have different shapes and sizes. Several investigators have revealed the surface texture of ferrospheres by scanning electron microscopy (SEM) ([Sokolar and Vodova, 2011](#)). The FS in fly ashes can be divided into

several types, namely, rough, smooth, polygon, dendritic, granular, and molten drop ferrospheres ([Zhao et al., 2006](#)).

Most FS have rough surfaces, with shapes close to an ideal sphere. [Sokol et al. \(2002\)](#) reported that most of the extracted FS from a Russian TPP were close to ideal spheres, with dendritic or skeletal morphology ([Sokol et al., 2002](#)). Rough-surfaced FS have depositions of numerous ferrous particles on their surface, which are crystalline in nature and have mixtures of magnetite, maghemite, and hematite. The size of these deposited ferrous particles varies from 50 to 200 nm. These deposited ferrous particles provide magnetic properties. Such types of ferrospheres are called rough-surfaced FS. In comparison to smooth-surfaced FS, rough-surfaced FS have higher magnetic strength.

Granular ferrospheres have a rough, porous, and granular surface structure and are often complicated by the additional presence of small granular crystals. The granular crystals on the surface of the ferrospheres are predominantly a result of iron oxide crystallization when the temperature decreases in the furnace of TPPs. [Yadav et al. \(2022a\)](#) reported the extraction of rough-surfaced FS with angular and granular deposits on their surface in CFA collected from TPPs in Kota, the SEM images of which are shown in [Figure 9](#).

Another type of ferrosphere is the smooth-surfaced type, with uniform depositions/distribution of ferrous on their surfaces. Due to this uniform distribution of ferrous, they have lower magnetic strength or are weakly magnetized. The diameter of smooth ferrospheres often varies from 40 to 60 μ . EDS and other instrumental analyses have shown low Fe content in smooth-surfaced ferrospheres. [Figure 10A](#) shows FESEM images of mixed, i.e., both smooth and rough-surfaced, FS. [Figure 10B](#) shows smooth-surfaced FS from [Yadav et al. \(2022b\)](#).

Polygon ferrospheres often exhibit blocky surface crystallites of iron oxides. Molten drop FS, with a great deal of goblet and granular particles on their surfaces, are formed during the crystallization of iron oxides from the liquid melt of the inner particles ([Fomenko et al., 2021](#)). A team led by Vu reported SEM images of magnetic and non-magnetic fractions of ferrospheres from CFA collected from

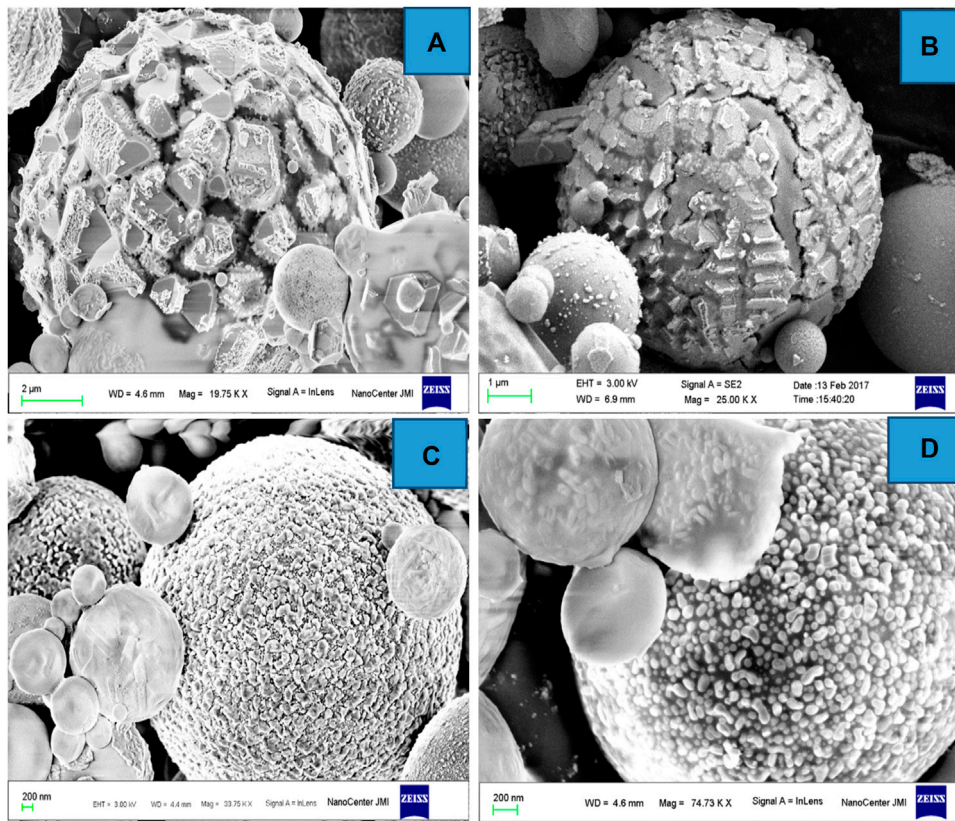


FIGURE 9
 FESEM micrographs of ferrospheres. (A) Angular deposits. (B) Crystalline pattern. (C) Spherule deposits. (D) Minute spherule deposits. Adapted from Yadav et al. (2022b).

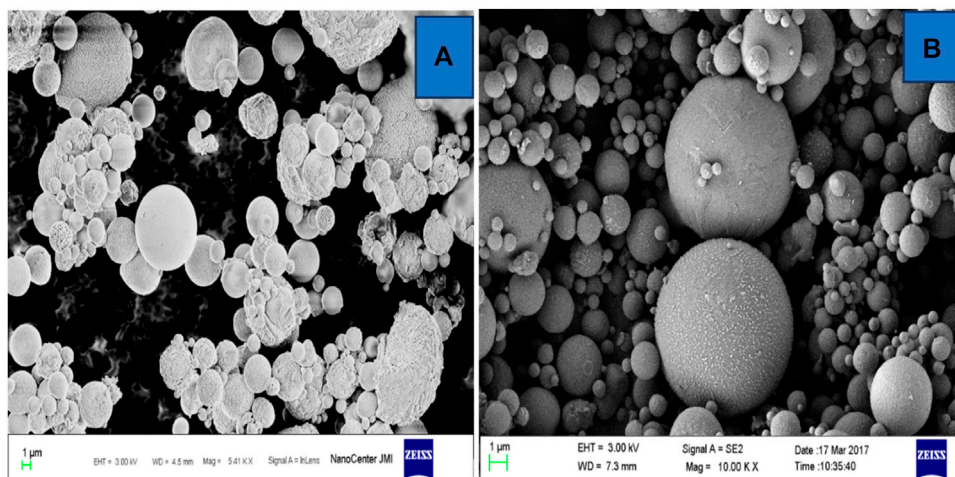


FIGURE 10
 FESEM micrographs of fly ash rough and smooth ferrospheres (A,B). Adapted from Yadav et al. (2022b).

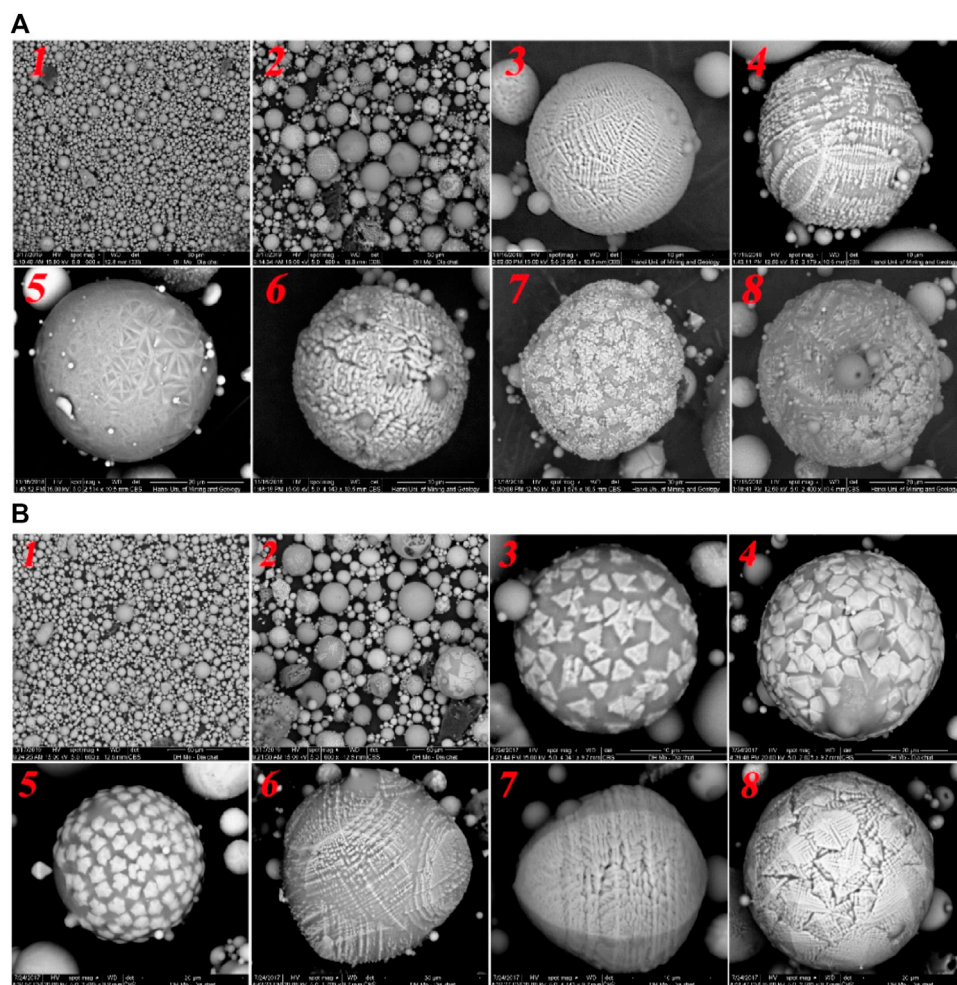


FIGURE 11

SEM micrographs of nonmagnetic 1 and magnetic particles (2–8) (A,B) collected from Uong Bi and Pha Lai fly ash. Adapted from Vu et al. (2019).

two different TPPs in Vietnam, as shown in Figure 11 (Vu et al., 2019).

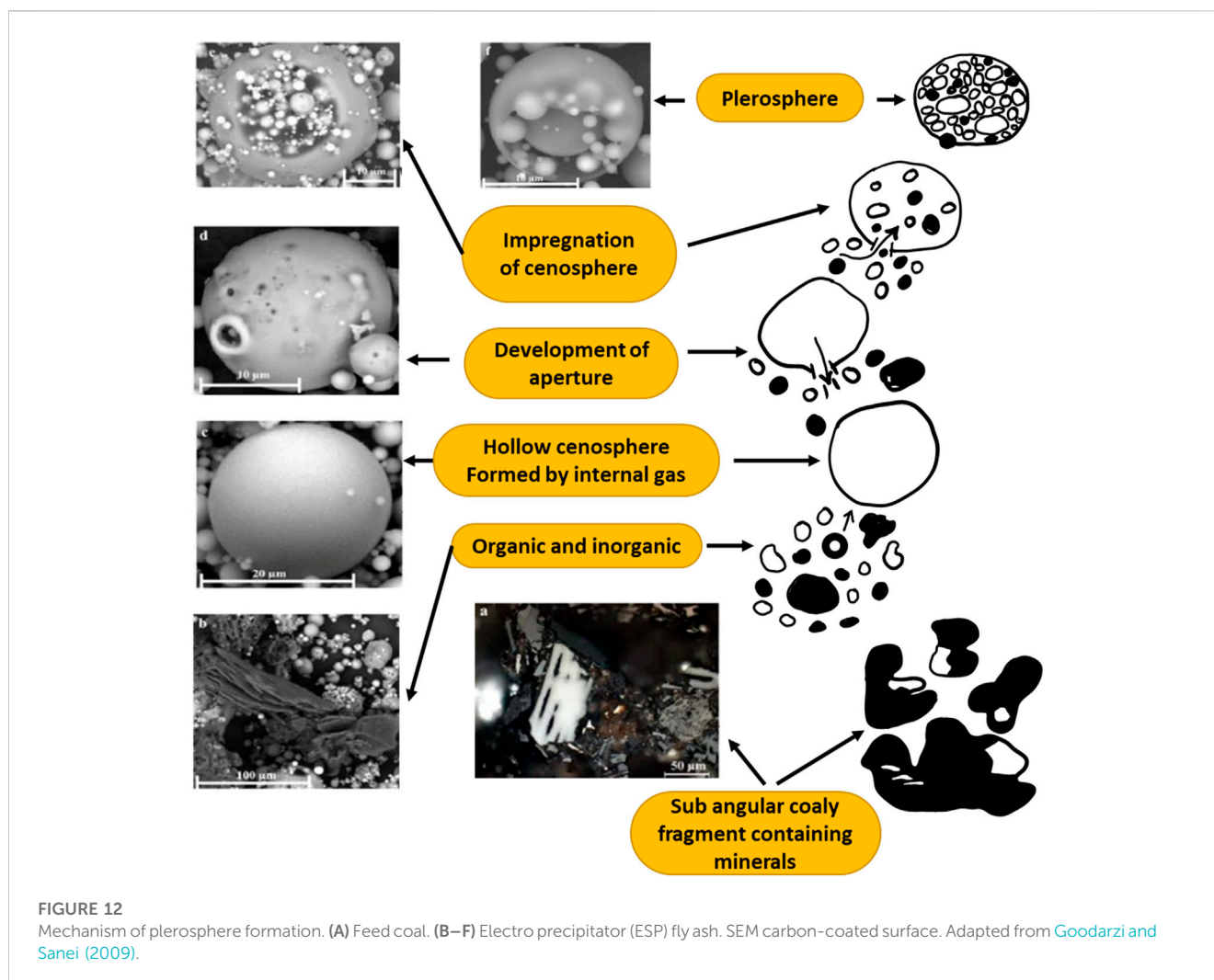
4 Mechanisms of ferrosphere and plerosphere formation in CFA

In addition to ferrospheres, CFA ferrous fractions also have plerospheres, which are hollow encapsulated spherical CFA particles filled with minerals and gases. CFA also contains cenospheres, which are spherical-shaped Al- and Si-rich particles with sizes varying from 5 to 50 μ (Yadav et al., 2020a).

4.1 Mechanism of plerosphere formation in CFA

Generally, CFA has both cenospheres and plerospheres; in such CFA, only a small portion of the cenospheres may be transformed into secondary plerospheres. CS can be transformed into PS by one of the following mechanisms, as shown in Figure 12. During the

combustion of coal, various minerals in the coal decompose, including carbon, carbonates, or carbides. As a result, the CFA particles will expand to stable CS. Due to this, the internal pressure of the CS will increase, followed by the formation of an aperture in the over-expanded CS, which releases the gas once its wall is punctured. Investigators have reported that puncture of the wall is possible due to collisions, which generate apertures of various sizes (Goodarzi and Sanei, 2009). During this step, CS that are ruptured are impregnated with microspheres that are confined within the cenosphere wall to form a secondary plerosphere. Which forces are behind the entry of CS into the MS is not clear. The finer particles may be trapped by the PS, which may be retained in the control devices of the TPPs; hence, such particles will be released into the air atmosphere at low concentrations. If PS and hollow CS have almost the same dimensions, the PS are heavier due to the additional weight of captured microspheres (Goodarzi and Sanei, 2009). Figure 12 shows the probable mechanism for the formation of plerospheres in CFA, as adapted from Chepaitis et al. (2011) and Goodarzi and Sanei (2009), respectively. According to Chepaitis et al. (2011), PS formation successively takes from a cenosphere; for instance, a CS particle in which the surface is weakened due to various



internal and external factors. The ruptured spherical particle from the previous step is filled with numerous smaller spherical particles, mineral fragments, and gases from the surroundings. This mechanism is common for the formation of both thick and thin-walled PS from CFA. Goodarzi and Sanei also reported a detailed mechanism for the formation of plerospheres in CFA (Goodarzi and Sanei, 2009).

5 Formation of ferrospheres in CFA

Coal contains pyrite and other sources of iron, which are used for the production of electricity in TPPs (Waanders et al., 2003). The high temperature of the furnace melts these organic and inorganic ferrous contents and forms a molten slag. This molten slag undergoes condensation and acquires a spherical shape while descending in the furnace (Guzmán-Carrillo et al., 2018). The preformed matrix has mainly Al and Si along with carbon, while iron is deposited on the surface of the preformed spheres. The deposition of granular iron on the surface of preformed spheres leads to rough-surfaced ferrospheres. This type of magnetic sphere is strongly magnetic. The other type of ferrosphere is the smooth type,

in which the ferrous and nonferrous melt, attaining a spherical shape. In this type of sphere, the ferrous particles are evenly distributed in the spheres; however, the spheres are weakly magnetized (Sunjidmaa et al., 2019).

Sokol et al. (2002) described the mechanism of formation of FS in TPPs in Russian Chelyabinsk. The authors suggested that during the combustion of fuel, high ferrous melts arise from the melting of the ferrous carbonates of coal. The confirmation of this supposition was strengthened by the increased content of P and Mn in the siderite and ankerite and FS. The chemical composition of each melt or final FS is determined by the chemical composition of Fe carbonate having admixtures of pelitic material. If the heating temperature is $>1,000^{\circ}\text{C}$, a considerable amount of Na and small amounts of K and Si are volatilized. Therefore, drops of ferrous melts have reduced amounts of Na, Si, and K and are enriched for Fe compared to the initial material (Sokol et al., 2002).

These iron melts have iron in the form of Fe^0 , Fe^{2+} , and ferrite complexes $(\text{Fe}^{3+} \text{O}_2)^-$ and $(\text{Fe}^{3+} \text{O}_5)^4-$. The Fe melts exist only under extremely reducing conditions as a proper phase in silicate liquid. When the furnace temperature is $> 1,200^{\circ}\text{C}$, there will be minimal fugacity of O_2 . The major fraction of FS is ferrispinel and silicate glass instead of native Fe or ferrosilicon. Hence, the formation of

such FS proceeds under conditions of higher partial oxygen pressure. Furthermore, the minerals of Fe are mainly governed by the temperature of the furnace in TPPs. Moreover, temperature also plays a role in the amorphous and crystalline nature of the minerals associated with FS. Silicate liquids with ferrous iron appear during the melting of CFA material at 1,000–1,100°C. During CFA formation, ferrite liquid with surplus amounts of Fe³⁺ in the form of (FeO₂)⁻ and (Fe₂O₅)⁴⁻ anions mainly appear at temperatures >1,500°C (Strzałkowska, 2021).

Furthermore, the nature and phases of iron oxides in FS depend on the cooling history of ferrous melts. The stability of minerals depends on the temperature in FS. Moreover, the Fe oxidation state in the FS depends on oxygen concentration and temperature. In addition to these two, it also depends on several other factors inside the furnace. The crystallization of ferrispinel is also governed by the temperature, i.e., lower temperatures favor crystallization. The chemical composition of ferrispinel is determined by the bulk chemistry of the melt (Ca, Mg, Mn, and Si concentrations), temperature, quenching rate, and O₂ fugacity. The crystallization of iron oxides leads to the enrichment of Ca, Mg, Si, and Al in the melt (Sokol et al., 2002). Ngu et al. (2007) reported the numerical ratio between PS and CS in CFA collected from an Australian TPP. The investigators demonstrated that this ratio increased with increased typical diameter (D₀). Choo et al. (2020) also reported the effect of temperature on the shape, size, phase transformations, and thermal expansion of cenospheres in CFA collected from a Malaysian TPP.

6 Extraction of ferrous particles and plerospheres from CFA

6.1 Recovery of plerospheres

Although CFA contains structurally varied types of particles, the two most closely related are CS and PS. Since PS have numerous smaller microspheres inside them, they are considerably heavier than the hollow CS (Danish and Mosaberpanah, 2020). Thus, CS and PS could be easily separated by means of density gradation. One such economical, and the most common, method is centrifugation, in which the heavier particles (PS) settle earlier and the hollow (lighter) CS settle later. Therefore, CS can be collected by decanting the supernatant, while PS can be collected from the residue. The residual particles can be washed several times with water to obtain pure PS free from CS and FS. PS can also be collected using a cyclone, which applies centrifugal force.

Since PS of same dimension as that of CS will be heavier due to the captured particles, it can be separated from the CFA slurry mixture by the centrifugal force generated in the cyclone. This is easier and more efficient if FS are first recovered using a magnet and then from nonferrous residue using cyclone. Hence, the heavier PS will be removed from the stream, while the lighter CS will remain in the stream of the cyclone. This is one way of enriching PS from a CFA sample, as reported by Goodarzi and Sanei (2009), who also reported the role of PS in reducing finer particles from TPPs.

Sharonova et al. (2003) reported the potential presence of PS in the magnetic microspheres in CFA. They further stated that it is very difficult to quantify the fractions of PS in close-cut fractions as the

outer wall can be continuous and, in this case, would screen the inner part of a globule. They found about 16% PS in the magnetic microspheres of CFA of Ekibastuz coal, with an Fe₂O₃ content of approximately 48%.

6.2 Extraction of ferrospheres from CFA

CFA ferrous fractions can be extracted by both wet slurry and dry magnetic separation methods. The dry separation method involves the formation of a slurry with water and extraction with the help of a strong magnet (Wrona et al., 2020). The dry separation involves the water-free based extraction of the ferrous fraction by conveyer belts. At one end of the conveyer belts, a strong magnet is attached to separate the magnetic fractions get from the nonmagnetic fractions (Valeev et al., 2019). Several investigators have reported the recovery of ferrous fraction from CFA by both dry and wet slurry separation processes (Petrus et al., 2011). The extraction of ferrous particles is possible by magnetic separation methods, which will also segregate ferrous from non-ferrous components.

The extracted ferrous particles can be further purified by treatment with various acids to synthesize pure iron oxides. Fomenko et al. (2021) reported the presence of magnetic fractions in CFA from Ekibastuz, with particulate matter sizes of about 2.5, 2.5–10, and 10 μ (Fomenko et al., 2021). Han et al. (2009) reported the recovery of magnetic fractions of CFA by wet slurry magnetic separation methods in coal bottom CFA. Yadav and Fulekar (2019) reported the extraction of ferrous fractions from CFA produced by TFFs in Gandhinagar by the wet slurry separation method. These were further transformed into four different phases of iron oxides by chemical and physical approaches. The size of the ferrospheres extracted from CFA was 0.2–7 μ, as revealed by FESEM and TEM (Yadav et al., 2023a; Yadav et al., 2023b). Sharonova et al. (2003) and Fomenko et al. (2002) also initially characterized FS in CFA and later extracted FS by applying dry and wet magnetic separation methods with varying efficiency from CFA of TPPs.

7 Applications of ferrospheres and plerospheres

7.1 Applications of ferrospheres

Ferrospheres extracted from CFA are chemically diverse due to the presence of Fe, Si, Al, C, K, Ca, Mg, etc., and are suitable for various applications, especially as catalysts in the petroleum industry, mainly in the high-temperature process of based oxidative dimerization of methane (Alterary and Marei, 2021; Naeem et al., 2022). FS are used frequently used in metallurgy for the extraction of pure iron particles. In metallurgy, FS are also used in steel industries for coke-smelting, and ore and coal dressing. Some examples in the literature have demonstrated the use of FS recovered from CFA as fillers for composite materials, which have gained significant attention (Zhao et al., 2006). FS are used as an alternative source of ferrous materials due to their high ferrous content (Dindi et al., 2019). FS are used as a raw material for iron-based industries. FS have also been widely used for the preparation

of nanocomposites for various applications, as reported by Yadav et al. (2021a). They are also used in concrete and ceramics applications like dense concrete production and nanoceramics (Nakonieczny et al., 2020).

Several investigators have used CFA ferrospheres as an adsorbent for the removal of dyes and other inorganic pollutants from wastewater. Fomenko (1998) demonstrated the application of FS extracted from TPPs as a catalyst for the high-temperature oxidative conversion of CH₄ (Anshits et al., 2021).

Moreover, recently they have been used in metallurgical processes; for instance, for the recovery and synthesis of iron oxide particles. Yadav (2019) reported the synthesis of four different iron oxide particles (IOPs); i.e., magnetite, maghemite, hematite, and ferrous carbonate by using CFA ferrospheres. Here, the ferrospheres were used as a raw material or source of iron, which was treated with concentrated mineral acids along with sonication at optimized temperatures. The ferrous leachate was used as a precursor material for the synthesis of IOPs by chemical co-precipitation using NaOH as a precipitating agent. Initially, ferrous carbonate was synthesized, which was later transformed into other phases of IOPs by chemical and calcination at 500–700°C (Yadav and Fulekar, 2020).

More recently, Yadav et al. (2022a) extracted ferrospheres from CFA collected from an Indian TPP. The collected FS were then treated with strong mineral acids (sulfuric acid and HCl) under sonication for 90 min along with heating at 60°C. Finally, the investigators developed surface-modified FS as a result of etching by acids. These surface-modified FS were used to remove Azure A dye from aqueous solutions. Approximately 25.03% of the dye was removed within 30 min (Yadav et al., 2022a).

7.2 Applications of plerospheres

7.2.1 Reduction of pollution in the atmosphere

Plerospheres are used in civil engineering applications and road construction, in ceramics and glass industries, and as a cementing material. The literature has shown that PS could be used for the remediation of pollutants from wastewater. Another underestimated application of PS is that they trap ultrafine particles from TPPs, making them part of the bottom ash and preventing their release into the atmosphere to cause air pollution (Wang et al., 2004). Plerospheres play an important role in reducing the production of fine CFA particles from coal-based power plants. Fine particulate matter (<2.5 μ) emitted from coal-based power plants are hazardous to environmental and human health. These fine particles may cause cardiovascular and respiratory disorders (Schraufnagel, 2020). Air filters fail to capture these particles; thus, they disperse into the environment and remain suspended for a longer duration, depending on their density in the air. Such particles can travel longer distances and, thus, have a larger spatial impact. Therefore, it is of utmost priority to reduce the emission of such particles during combustion. Goodarzi and Sanei suggested that the formation of large plerosphere particles is one possible solution to capture smaller CFA particles. During combustion, plerospheres encapsulate finer particles and are later captured by particle control devices such as ESP or fabric filters (Goodarzi and Sanei, 2009; Schraufnagel, 2020).

7.2.2 Plerospheres in aerospace applications

Due to the unique properties of PS, they are commonly used to prepare composites used in aerospace applications due to their light weight and high mechanical strength. Nowadays, ultrafine PS are used to fill the phenolic matrix to produce an AO-resistant fiber/phenolic resin composite. Such PS do not react with atomic oxygen. Investigations have shown that the use of PS as fillers provides considerable protection to the fiber/phenolic resin against AO erosion (Wang et al., 2004; Qian and Xuan, 2018).

7.2.3 Plerospheres for the removal of air pollutants

CFA associated with different chemical constituents is used to efficiently resolve environmental problems such as air pollution. CFA contents could be used as an economical sorbent for flue gas purification and air cleaning. The primary components of CFA, such as silica, alumina, and oxides of Fe, have been employed for the removal of trace elements and environmental SO_x or NO_x gases. Sulfur oxides and nitrogen oxides cause acid rain and have become a serious problem for the environment. Thus, many researchers are motivated to use CFA mixed with other minerals such as CaO or Ca(OH)₂. Allen and Hayhurst (1996) used CaO to minimize SO₂ production, producing CaSO₄, which is comparably less cost-effective than the wet and semi-dry processes for desulfurization. Additionally, CFA has been explored as a cheap sorbent material for flue gas desulfurization either in pure or mixed form with desired minerals. Ca(OH)₂ mixed with CFA has been studied for increased efficiency of SO₂ adsorption, while CaO has been applied to treat SO₂ in water (at room temperature) as a low-cost desulfurization method by Li et al. (2017). Similarly, activated carbon has been widely used to adsorb heavy metal elements from wastewater; however, its limited availability is a major issue for its extensive use. Therefore, CFA has been converted as an effective adsorbent and employed as an economically desired material for the remediation of toxic substances from industries, laboratories, and wastewater. Gupta and Sharma (2003) used bagasse CFA (sugar industries waste) to clean Zn ions from water by evaluating the kinetic rate of adsorption. The active surface sites of the ferrosphere permit stronger chemisorption due to the larger area, which explains the adsorption effects. However, the porous nature of the outer surface also contributes to adsorbing organic and inorganic molecules or elements during water or air cleaning. Particle diffusion and accumulation on the porous structure have gained considerable attention in CFA extraction and its importance in purification chemistry. External and internal transport occur by involving both open-surface sites and porous structures. The kinetics of adsorption are often rapid; thus, many theoretical approaches have been employed to investigate the rate-determining steps.

In this regard, a modified procedure was adopted by Decker and Klabunde (1996) and Yang et al., in which around 4% of Fe₂O₃ was mixed with CaO to adsorb SO₂ (Georgiadis et al., 2020). They found almost double reactivity for the adsorption due to the use of combined CaO/Fe₂O₃, and reported it as a destructive adsorbent for sulfur dioxides. The FS and other constituents were identified as suitable destructive agents for toxins, including chlorinated hydrocarbons such as CHCl₃, CCl₄, C₂Cl₄, C₂HCl₃, and acid gases (SO₂, CO₂, HCl, and SO₃). Spherical and narrow particles show specific reactivities toward toxins, resulting in a cost-effective technique for air and water treatments using CFA and its derivatives. Organic dyes are also degraded by waste material-bottom ash. The concentration of adsorbents and treatment time play crucial roles in the adsorption kinetics. The same evidence was addressed by

Gupta et al. (2008). The heterocyclic and aromatic compounds removed by utilizing such CFA derivatives and a wider research potential were highlighted in this sector. To investigate the geometric and physicochemical features of CFA/particles, Peloso et al. removed toluene vapor using CFA particles (Peloso et al., 1983). A satisfactory performance for toluene adsorption was obtained due to the chemical activation, total porosity, and specific surface area of the sorbent. Furthermore, the adsorption kinetics of volatile aromatic hydrocarbons and *x*-xylene were investigated by Rothenberg et al. (1991), who showed that the reactivity on pore structure was impactful for adsorbing these organic substances in gaseous form. The adsorption rate is mainly regulated by the diffusion process, while the partitioning of gaseous aromatic compounds depends upon the particle sizes, vapor pressure, temperatures, etc. Therefore, by utilizing such CFAs and their derived value-added minerals, various environmental issues could be resolved to make human lives healthier and easier by minimizing carcinogenic and mutagenic effects (caused by heterocyclic/aromatic toxic contents) by controlling air and water quality (Umejuru et al., 2021).

7.2.4 Applications of ferrospheres and plerospheres in defense systems

Several reports have described the use of the whole CFA or its components separately for defense and military purposes. CFA-based civil products like bricks and blocks are light in weight and can be directly used for the rapid construction of army base camps. Moreover, the light weight allows easy transportation (Varshney et al., 2022). Additionally, CFA-based bricks require less water during building or construction; thus, they are beneficial for army personnel for utilization in hilly or desert areas with limited water present. Due to the presence of ferrous particles, cenospheres, and plerospheres, this could be used as a material with high mechanical strength. It is used as a filler in several army-utilizable products. Additionally, the separate components, such as FS, have been used for the development of magnetic-based materials due to their magnetic properties. The most widely used particles are CS, which are very lightweight, with high mechanical strength and excellent electromagnetic properties. Both PS and CS are commonly used in defense radar systems due to their electromagnetic (EM) properties and are also being used as a substitute for CNTs in the development of lightweight materials in aircrafts. Various nanocomposites developed using CFA products have also been used for military purposes (Yadav and Fulekar, 2019; Yadav and Pandita, 2019; Yadav et al., 2020b).

CFA or cenospheres, plerospheres, and ferrospheres could also be used for the detection of toxic or radioactive substances by surface functionalizing of these particles to act as sensing materials. CFA-based products could be coated with specific chemicals for the detection of any chemical gases released by an enemy army. Moreover, cenospheres, ferrospheres, and plerospheres could be used by the army as sensing or detection agents in tunnels where chemical weapons, hazardous gases, or any liquid chemicals might have been placed by an enemy army (Choudhary et al., 2020; Yadav et al., 2021b).

8 Conclusion

Due to the variation in temperature of the furnace in thermal power plants, different zones are created. Consequently, morphologically different CFA structures are formed; i.e., ferrospheres, cenospheres,

and plerospheres, which are mainly nearly spherical in shape. These spherical structures vary in their chemical composition and inner or outer structures. Although coal is a mixture of organic and inorganic compounds, it is dominated by organic compounds which, upon decomposition, produce these spherical structures. Among these spherical structures, ferrous-rich ferrospheres exhibit magnetic properties due to the depositions of iron oxides on their surfaces. These deposited iron oxides are mainly crystalline in nature, belonging to magnetite, maghemite, and hematite phases. Among these spheres, ferrospheres show maximum diversity, including rough, smooth, polygon, dendritic, granular, or molten drop, and range in size from a few nanometers to several microns. The fly ash extracted from unmodified ferrospheres has applications in metallurgy, ore dressing, and catalysis. Plerospheres are double-layered solid spherical particles, in which the outer and larger spheres trap numerous microspheres or mineral fragments. Based on the plerosphere wall thickness, it is categorized as thin- or thick-walled. The thickness of plerospheres is due to the coating of minerals or carbon at higher temperatures in the furnace. Plerospheres are used in engineering, military, ceramics, and wastewater treatment applications due to their unique and remarkable properties.

Author contributions

VY, NC, GI, SW, TM, and AG: original draft, manuscript writing and review, data curation, formal analysis, and investigation. MA, KY, M-KJ, B-HJ, and AA: conceptualization, validation, manuscript writing and review, software, visualization, project administration, and funding acquisition. VY, B-HJ, and TM, supervision, methodology, and resources. All authors contributed to the article and approved the submitted version.

Acknowledgments

The authors extend their appreciation to the Deanship of Scientific Research at King Khalid University (KKU) for funding this research through the Research Group Program Under the Grant Number: (R.G.P.2/513/44). This work was supported by the Mid-Career Researcher Program (grant no. 2020RIA2C3004237) through the National Research Foundation of the Republic of Korea.

Conflict of interest

The authors declare that the research was conducted in the absence of any commercial or financial relationships that could be construed as a potential conflict of interest.

Publisher's note

All claims expressed in this article are solely those of the authors and do not necessarily represent those of their affiliated organizations, or those of the publisher, the editors, and the reviewers. Any product that may be evaluated in this article, or claim that may be made by its manufacturer, is not guaranteed or endorsed by the publisher.

References

- Adesina, A. (2020). Sustainable application of cenospheres in cementitious materials – overview of performance. *Dev. Built Environ.* 4, 100029. doi:10.1016/j.dibe.2020.100029
- Alam, J., Yadav, V. K., Yadav, K. K., Cabral-Pinto, M. M. S., Tavker, N., Choudhary, N., et al. (2021). Recent advances in methods for the recovery of carbon nanominerals and polyaromatic hydrocarbons from coal fly ash and their emerging applications. *Cryst. (Basel)* 11, 88–24. doi:10.3390/cryst11020088
- Allen, D., and Hayhurst, A. N. (1996). Reaction between gaseous sulfur dioxide and solid calcium oxide mechanism and kinetics. *J. Chem. Soc. Faraday Trans.* 92, 1227–1238. doi:10.1039/FT9969201227
- Alterary, S. S., and Marei, N. H. (2021). Fly ash properties, characterization, and applications: A review. *J. King Saud. Univ. Sci.* 33, 101536. doi:10.1016/j.jksus.2021.101536
- Anshits, N. N., Fedorchak, M. A., Zhizhaev, A. M., Sharonova, O. M., and Anshits, A. G. (2018). Composition and structure of block-type ferrospheres isolated from calcium-rich power plant ash. *Inorg. Mater.* 54, 187–194. doi:10.1134/S0020168518020012
- Anshits, N. N., Fomenko, E. v., and Anshits, A. G. (2021). Composition–structure relationship and routes of formation of blocklike ferrospheres produced by pulverized combustion of two coal types. *ACS Omega* 6, 26004–26015. doi:10.1021/acsomega.1c02880
- Balapur, M., Thway, T., Rao, R., Moser, N., Garboczi, E. J., Hsuan, Y. G., et al. (2022). A thermodynamics-guided framework to design lightweight aggregate from waste coal combustion fly ash. *Resour. Conserv. Recycl.* 178, 106050. doi:10.1016/j.resconrec.2021.106050
- Baziak, A., Plawecka, K., Hager, I., Castel, A., and Korniejenko, K. (2021). Development and characterization of lightweight geopolymer composite reinforced with hybrid carbon and steel fibers. *Materials* 14, 5741. doi:10.3390/ma14195741
- Birla, S., Mondal, D. P., Das, S., Kashyap, D. K., and Ch, V. A. N. (2017). Effect of cenosphere content on the compressive deformation behaviour of aluminum-cenosphere hybrid foam. *Mater. Sci. Eng. A* 685, 213–226. doi:10.1016/j.msea.2016.12.131
- Blissett, R. S., and Rowson, N. A. (2012). A review of the multi-component utilisation of coal fly ash. *Fuel* 97, 1–23. doi:10.1016/j.fuel.2012.03.024
- Chepaitis, P. S., Millette, J. R., and Wood, T. B. V. (2011). A novel coal fly ash sphere reveals a Complete understanding of Plerosphere Formation. *Microscope* 59, 175–180.
- Choo, T. F., Salleh, M. A. M., Kok, K. Y., Matori, K. A., and Rashid, S. A. (2020). Effect of temperature on morphology, phase transformations and thermal expansions of coal fly ash cenospheres. *Cryst. (Basel)* 10, 1–11. doi:10.3390/cryst10060481
- Choudhary, N., Yadav, V. K., Malik, P., Khan, S. H., Inwati, G. K., Suriyaprabha, R., et al. (2020). “Recovery of natural nanostructured minerals: Ferrospheres, plerospheres, cenospheres, and carbonaceous particles from fly ash,” in *Handbook of research on emerging developments and environmental impacts of ecological chemistry*. (Hershey, PA: IGI Global), 450–470.
- Danish, A., and Mosaberpanah, M. A. (2020). Formation mechanism and applications of cenospheres: A review. *J. Mater. Sci.* 55, 4539–4557. doi:10.1007/s10853-019-04341-7
- Das, T., Boruah, P. K., Das, M. R., and Saikia, B. K. (2016). Formation of onion-like fullerene and chemically converted graphene-like nanosheets from low-quality coals: Application in photocatalytic degradation of 2-nitrophenol. *RSC Adv.* 6, 35177–35190. doi:10.1039/C6RA04392E
- Decker, S., and Klabunde, K. J. (1996). Enhancing effect of Fe₂O₃ on the ability of nanocrystalline calcium oxide to adsorb SO₂. *J. Am. Chem. Soc.* 118, 12465–12466. doi:10.1021/ja962371e
- Dindi, A., Quang, D. V., Vega, L. F., Nashef, E., and Abu-Zahra, M. R. M. (2019). Applications of fly ash for CO₂ capture, utilization, and storage. *J. CO₂ Util.* 29, 82–102. doi:10.1016/j.jcou.2018.11.011
- dos Santos, R. P., Martins, J., Gadelha, C., Cavada, B., Albertini, A. V., Arruda, F., et al. (2014). Coal fly ash ceramics: Preparation, characterization, and use in the Hydrolysis of sucrose. *Sci. World J.* 2014, 154651–154657. doi:10.1155/2014/154651
- Eisele, T. C., and Kawatra, S. K. (2002). Use of froth flotation to remove unburned carbon from fly ash. *Mineral Process. Extr. Metallurgy Rev.* 23, 1–10. doi:10.1080/08827500214516
- Ferrari, S. F., Cardoso, A. M., Paprocki, A., and Pires, M. (2016). Integrated synthesis of zeolites using coal fly ash: Element distribution in the products, washing waters and effluent. *J. Braz. Chem. Soc.* 27, 2034–2045. doi:10.5935/0103-5053.20160093
- Fisher, G. L., Chang, D. P. Y., and Brummer, M. (1976). Fly ash collected from electrostatic precipitators: Microcrystalline structures and the mystery of the spheres. *Sci.* (1979) 192, 553–555. doi:10.1126/science.192.4239.553
- Fomenko, E. V., Anshits, N. N., Pankova, M. V., Solovyov, L. A., and Anshits, A. G. (2011). “Fly ash cenospheres: Composition, morphology, structure, and helium permeability,” in *World of coal ash (WOCA) conference* (Denver, USA). Available at: <http://www.flyash.info/>.
- Fomenko, E. v., Anshits, N. N., Solovyov, L. A., Knyazev, Y. v., Semenov, S. v., Bayukov, O. A., et al. (2021). Magnetic fractions of PM_{2.5}, pm_{2.5–10}, and PM₁₀ from coal fly ash as environmental pollutants. *ACS Omega* 6, 20076–20085. doi:10.1021/acsomega.1c03187
- Georgiadis, A. G., Charisiou, N. D., and Goula, M. A. (2020). Removal of hydrogen sulfide from various industrial gases: A review of the most promising adsorbing materials. *Catalysts* 10, 521. doi:10.3390/catal10050521
- Gnanamoorthy, G., Priya, P., Ali, D., Lakshmi, M., Yadav, V. K., and Varghese, R. (2021). A new CuZr₂S₄/rGO and their reduced graphene oxide nanocomposites enhanced photocatalytic and antimicrobial activities. *Chem. Phys. Lett.* 781, 139011. doi:10.1016/j.cplett.2021.139011
- Gollakota, A. R. K., Volli, V., and Shu, C. M. (2019). Progressive utilisation prospects of coal fly ash: A review. *Sci. Total Environ.* 672, 951–989. doi:10.1016/j.scitotenv.2019.03.337
- Goodarzi, F., and Sanei, H. (2009). Plerosphere and its role in reduction of emitted fine fly ash particles from pulverized coal-fired power plants. *Fuel* 88, 382–386. doi:10.1016/j.fuel.2008.08.015
- Guedes, A., and Valentim, B. (2021). Editorial for special issue “minerals and elements from fly ash and bottom ash as a source of secondary raw materials”. *Minerals* 11, 438. doi:10.3390/min11050438
- Gupta, V. K., and Sharma, S. (2003). Removal of zinc from aqueous solutions using bagasse fly ash – a low cost adsorbent. *Ind. Eng. Chem. Res.* 42, 6619–6624. doi:10.1021/ie0303146
- Gupta, V. K., Mittal, A., Gajbe, V., and Mittal, J. (2008). Adsorption of basic fuchsin using waste materials—Bottom ash and deoiled soya—As adsorbents. *J. Colloid Interface Sci.* 319, 30–39. doi:10.1016/j.jcis.2007.09.091
- Gupta, N., Yadav, V. K., Yadav, K. K., Alwetaishi, M., Gnanamoorthy, G., Singh, B., et al. (2022). Recovery of iron nanominerals from sacred incense sticks ash waste collected from temples by wet and dry magnetic separation method. *Environ. Technol. Innov.* 25, 102150. doi:10.1016/j.eti.2021.102150
- Guzmán-Carrillo, H. R., Pérez, J. M., Aguilar Reyes, E. A., and Romero, M. (2018). Coal fly ash and steel slag valorisation throughout a vitrification process. *Int. J. Environ. Sci. Technol.* 15, 1757–1766. doi:10.1007/s13762-017-1542-5
- Han, G.-C., Um, N.-I., You, K.-S., Cho, H.-C., and Ahn, J.-W. (2009). Recovery of ferromagnetic material by wet magnetic separation in coal bottom ash. *Geosystem Eng.* 12, 9–12. doi:10.1080/12269328.2009.10541292
- Haustein, E., and Kuryłowicz-Cudowska, A. (2020). The effect of fly ash micro-spheres on the pore structure of concrete. *Minerals* 10, 58. doi:10.3390/min10010058
- Kaasik, M., Alliksaar, T., Ivask, J., and Loosaar, J. (2005). Spherical fly ash particles from oil shale fired power plants in atmospheric precipitations. Possibilities of quantitative tracing. *Oil Shale* 22, 547–562.
- Kanhar, A. H., Chen, S., and Wang, F. (2020). Incineration fly ash and its treatment to possible utilization: A review. *Energies (Basel)* 13, 6681. doi:10.3390/en13246681
- Khoshnoud, P., and Abu-Zahra, N. (2015). Effect of cenosphere fly ash on the thermal, mechanical, and morphological properties of rigid PVC foam composites. *J. Res. Updat. Polym. Sci.* 4, 1–14. doi:10.6000/1929-5995.2015.04.01.1
- Kolay, P. K., and Singh, D. N. (2001). Physical, chemical, mineralogical, and thermal properties of cenospheres from an ash lagoon. *Cem. Concr. Res.* 31, 539–542. doi:10.1016/S0008-8846(01)00457-4
- Kutchko, B. G., and Kim, A. G. (2006). Fly ash characterization by SEM–EDS. *Fuel* 85, 2537–2544. doi:10.1016/j.fuel.2006.05.016
- Li, X.-Y., Jiang, Y., Liu, X.-Q., Shi, L.-Y., Zhang, D.-Y., and Sun, L.-B. (2017). Direct synthesis of zeolites from a natural clay, attapulgite. *ACS Sustain. Chem. Eng.* 5, 6124–6130. doi:10.1021/acssuschemeng.7b01001
- Liu, D., Duan, Y. Y., Yang, Z., and Yu, H. T. (2014). A new route for unburned carbon concentration measurements eliminating mineral content and coal rank effects. *Sci. Rep.* 4, 4567. doi:10.1038/srep04567
- Liu, H., Sun, Q., Wang, B., Wang, P., and Zou, J. (2016). Morphology and composition of microspheres in fly ash from the luohuang power plant, Chongqing, Southwestern China. *Minerals* 6, 30. doi:10.3390/min6020030
- Liu, F., Liu, H. Q., Wei, G. X., Zhang, R., Zeng, T. T., Liu, G. S., et al. (2018). Characteristics and treatment methods of medical waste incinerator fly ash: A review. *Processes* 6, 173. doi:10.3390/pr6100173
- Lv, B., Jiao, F., Chen, Z., Dong, B., Fang, C., Zhang, C., et al. (2022). Separation of unburned carbon from coal fly ash: Pre-classification in liquid–solid fluidized beds and subsequent flotation. *Process Saf. Environ. Prot.* 165, 408–419. doi:10.1016/j.psep.2022.07.031
- Marinina, O., Nevskaya, M., Jonek-Kowalska, I., Wolniak, R., and Marinin, M. (2021). Recycling of coal fly ash as an example of an efficient circular economy: A stakeholder approach. *Energies (Basel)* 14, 3597. doi:10.3390/en14123597

- Markandeya, M., Shukla, S. P., and Srivastav, A. L. (2021). Removal of Disperse Orange and Disperse Blue dyes present in textile mill effluent using zeolite synthesized from cenospheres. *Water Sci. Technol.* 84, 445–457. doi:10.2166/wst.2021.216
- Mohammed, S. A., Koting, S., Katman, H. Y. B., Babalghaith, A. M., Patah, M. F. A., Ibrahim, M. R., et al. (2021). A review of the utilization of coal bottom ash (Cba) in the construction industry. *Sustain.* 13, 8031. doi:10.3390/su13148031
- Naeem, N., Khoja, A. H., Butt, F. A., Arfan, M., Liaquat, R., and Hasnat, A. U. (2022). Partial oxidation of methane over biomass fly ash (BFA)-supported Ni/CaO catalyst for hydrogen-rich syngas production. *Res. Chem. Intermed.* 48, 2007–2034. doi:10.1007/s11164-022-04685-x
- Nakonieczny, D. S., Antonowicz, M., and Paszenda, Z. K. (2020). Cenospheres and their application advantages in biomedical engineering - a systematic review. *Rev. Adv. Mater. Sci.* 59, 115–130. doi:10.1515/rams-2020-0011
- Ngu, L., Wu, H., and Zhang, D. (2007). Characterization of ash cenospheres in fly ash from Australian power stations. *Energy & Fuels* 21, 3437–3445. doi:10.1021/ef700340k
- Noor-ul-Amin, N. I. J. A. (2014). A multi-directional utilization of different ashes. *RSC Adv.* 4, 62769–62788. doi:10.1039/C4RA06568A
- Peloso, A., Rovatti, M., and Ferraiolo, G. (1983). Fly ash as adsorbent material for toluene vapours. *Resour. Conserv. Int.* 2, 211–220. doi:10.1016/0166-3097(83)90015-9
- Petrus, H. T. B. M., Hirajima, T., Oosako, Y., Nonaka, M., Sasaki, K., and Ando, T. (2011). Performance of dry-separation processes in the recovery of cenospheres from fly ash and their implementation in a recovery unit. *Int. J. Min. Process* 98, 15–23. doi:10.1016/j.minpro.2010.09.002
- Qian, M., and Xuan, X. Y. (2018). Hyperthermal atomic oxygen durable transparent silicon-reinforced polyimide. *High. Perform. Polym.* 31, 831–842. doi:10.1177/0954008318802939
- Rothenberg, S. J., Mettler, G., Poliner, J., Bechtold, W. E., Eidson, A. F., and Newton, G. J. (1991). Adsorption kinetics of vapor-phase m-xylene on coal fly ash. *Environ. Sci. Technol.* 25, 930–935. doi:10.1021/es00017a016
- Schraufnagel, D. E. (2020). The health effects of ultrafine particles. *Exp. Mol. Med.* 52, 311–317. doi:10.1038/s12276-020-0403-3
- Sharonova, O., Anshits, N., and Akimochkina, G. (2003). Composition and morphology of magnetic microspheres in power plant fly ash of coal from the Ekibastuz and Kuznetsk basins. *Chem. Sustain. Dev.* 11, 639–648. Available at: <https://www.researchgate.net/publication/292796411>.
- Sharonova, O. M., Anshits, N. N., Fedorchak, M. A., Zhizhaev, A. M., and Anshits, A. G. (2015). Characterization of ferrospheres recovered from high-calcium fly ash. *Energy & Fuels* 29, 5404–5414. doi:10.1021/acs.energyfuels.5b01618
- Shoumkova, A. S. (2011). Magnetic separation of coal fly ash from Bulgarian power plants. *Waste Manag. Res.* 29, 1078–1089. doi:10.1177/0734242X10379494
- Snellings, R., Kazemi-Kamyab, H., Nielsen, P., and van den Abeele, L. (2021). Classification and milling increase fly ash pozzolanic reactivity. *Front. Built Environ.* 7, 44. doi:10.3389/fbuil.2021.670996
- Sokol, E. v., Kalugin, V. M., Nigmatulina, E. N., Volkova, N. I., Frenkel, A. E., and Maksimova, N. V. (2002). Ferrospheres from fly ashes of Chelyabinsk coals: Chemical composition, morphology and formation conditions. *Fuel* 81, 867–876. doi:10.1016/S0016-2361(02)00005-4
- Sokolar, R., and Vodova, L. (2011). The effect of fluidized fly ash on the properties of dry pressed ceramic tiles based on fly ash-clay body. *Ceram. Int.* 37, 2879–2885. doi:10.1016/j.ceramint.2011.05.005
- Song, C., Ren, K., Long, S., Zhu, Y., Teng, Z., Wang, M., et al. (2021). Preparation of activated carbon from unburned carbon in biomass fly ash and its supercapacitor performance. *J. Fuel Chem. Technol.* 49, 1936–1942. doi:10.1016/S1872-5813(21)60129-9
- Strzałkowska, E. (2021). Morphology and chemical composition of mineral matter present in fly ashes of bituminous coal and lignite. *Int. J. Environ. Sci. Technol.* 18, 2533–2544. doi:10.1007/s13762-020-03016-0
- Sunjidmaa, D., Batdemberel, G., and Takibai, S. (2019). A study of ferrospheres in the coal fly ash. *Open J. Appl. Sci.* 09, 10–16. doi:10.4236/ojapps.2019.91002
- Tiwari, M. K., Bajpai, S., Dewangan, U. K., and Tamrakar, R. K. (2015). Suitability of leaching test methods for fly ash and slag: A review. *J. Radiat. Res. Appl. Sci.* 8, 523–537. doi:10.1016/j.jrras.2015.06.003
- Tiwari, A. J., Ashraf-Khorassani, M., and Marr, L. C. (2016). C60 fullerenes from combustion of common fuels. *Sci. Total Environ.* 547, 254–260. doi:10.1016/j.scitotenv.2015.12.142
- Um, N., and Jeon, T.-W. (2021). Pretreatment method for the utilization of the coal ash landfilled in ash ponds. *Process Saf. Environ. Prot.* 153, 192–204. doi:10.1016/j.psep.2021.07.013
- Umejuru, E. C., Prabakaran, E., and Pillay, K. (2021). Coal fly ash decorated with graphene oxide-tungsten oxide nanocomposite for rapid removal of Pb(2+) ions and reuse of spent adsorbent for photocatalytic degradation of acetaminophen. *ACS Omega* 6, 11155–11172. doi:10.1021/acsomega.0c04194
- Valeev, D., Kunilova, I., Alpatov, A., Varnavskaya, A., and Ju, D. (2019). Magnetite and carbon extraction from coal fly ash using magnetic separation and flotation methods. *Minerals* 9, 320. doi:10.3390/min9050320
- Valentim, B., Shreya, N., Paul, B., Gomes, C. S., Sant'Ovaia, H., Guedes, A., et al. (2016). Characteristics of ferrospheres in fly ashes derived from Bokaro and Jharia (Jharkand, India) coals. *Int. J. Coal Geol.* 153, 52–74. doi:10.1016/j.coal.2015.11.013
- Varshney, A., Dahiya, P., Sharma, A., Pandey, R., and Mohan, S. (2022). Fly ash application in soil for sustainable agriculture: An Indian overview. *Energy Ecol. Environ.* 7, 340–357. doi:10.1007/s40974-022-00241-w
- Vereshchagina, T. A., Kutikhina, E. A., Solovyov, L. A., Vereshchagin, S. N., Mazurova, E. v., Chernykh, Y. Yu., et al. (2018). Synthesis and structure of analcime and analcime-zirconia composite derived from coal fly ash cenospheres. *Microporous Mesoporous Mater.* 258, 228–235. doi:10.1016/j.micromeso.2017.09.011
- Vu, D. H., Bui, H. B., Kalantar, B., Bui, X. N., Nguyen, D. A., Le, Q. T., et al. (2019). Composition and morphology characteristics of magnetic fractions of coal fly ash wastes processed in high-temperature exposure in thermal power plants. *Appl. Sci. Switz.* 9, 1964. doi:10.3390/app9091964
- Waanders, F. B., Vinken, E., Mans, A., and Mulaba-Bafubandi, A. F. (2003). Iron minerals in coal, weathered coal and coal ash – SEM and mössbauer results. *Hyperfine Interact.* 148, 21–29. doi:10.1023/B:HYPE.0000003760.89706.f6
- Wang, M., Shen, Z., Cai, C., Ma, S., and Xing, Y. (2004). Experimental investigations of polypropylene and poly(vinyl chloride) composites filled with plerospheres. *J. Appl. Polym. Sci.* 92, 126–131. doi:10.1002/app.13667
- Wang, T., Wang, K., Ye, F., Ren, Y., and Xu, C. (2021). Characterization and thermal properties of a shape-stable Na₂CO₃-K₂CO₃/coal fly ash/expanded graphite composite phase change materials for high-temperature thermal energy storage. *J. Energy Storage* 33, 102123. doi:10.1016/j.est.2020.102123
- Wrona, J., Zukowski, W., Bradlo, D., and Czupryński, P. (2020). Recovery of cenospheres and fine fraction from coal fly ash by a novel dry separation method. *Energies (Basel)* 13, 3576. doi:10.3390/en13143576
- Xue, Q. F., and Lu, S. G. (2008). Microstructure of ferrospheres in fly ashes: SEM, EDX and ESEM analysis. *J. Zhejiang Univ. Sci. A* 9, 1595–1600. doi:10.1631/jzus.A0820051
- Yadav, V. K., and Fulekar, M. H. (2014). Isolation and characterization of iron nanoparticles from coal fly ash from gandhinagar (Gujarat) thermal power plant (A mechanical method of isolation). *Int. J. Eng. Res.* 3. doi:10.17577/IJERTV3IS060628
- Yadav, V. K., and Fulekar, M. H. (2019). Green synthesis and characterization of amorphous silica nanoparticles from fly ash. *Mater. Today Proc.* 18, 4351–4359. doi:10.1016/j.matpr.2019.07.395
- Yadav, V. K., and Fulekar, M. H. (2020). Advances in methods for recovery of ferrous, alumina, and silica nanoparticles from fly ash waste. *Ceramics* 3, 384–420. doi:10.3390/ceramics3030034
- Yadav, V. K., and Pandita, P. R. (2019). “Fly ash properties and their applications as a soil ameliorant,” in *Amelioration technology for Soil sustainability*. Editor A. K. Rathoure (Hershey, PA, USA: IGI Global), 59–89. doi:10.4018/978-1-5225-7940-3.ch005
- Yadav, V. K., Choudhary, N., Khan, S. H., Malik, P., Inwati, G. K., Suriyaprabha, R., et al. (2020a). “Synthesis and characterization of nano-biosorbents and their applications for waste water treatment,” in *Handbook of research on emerging developments and environmental impacts of ecological chemistry*. (Hershey, PA: IGI Global), 252–290. doi:10.4018/978-1-7998-1241-8.ch012
- Yadav, V. K., Saxena, P., Lal, C., Gnanamoorthy, G., Choudhary, N., Singh, B., et al. (2020b). Synthesis and characterization of mullites from silicoaluminous fly ash waste. *Int. J. Appl. Nanotechnol. Res.* 5, 10–25. doi:10.4018/ijnanr.20200101.0a2
- Yadav, V. K., Gnanamoorthy, G., Cabral-Pinto, M. M. S., Alam, J., Ahamed, M., Gupta, N., et al. (2021a). Variations and similarities in structural, chemical, and elemental properties on the ashes derived from the coal due to their combustion in open and controlled manner. *Environ. Sci. Pollut. Res.* 28, 32609–32625. doi:10.1007/s11356-021-12989-5
- Yadav, V. K., Yadav, K. K., Tirth, V., Jangid, A., Gnanamoorthy, G., Choudhary, N., et al. (2021b). Recent advances in methods for recovery of cenospheres from fly ash and their emerging applications in ceramics, composites, polymers and environmental cleanup. *Cryst. (Basel)* 11, 1067. doi:10.3390/cryst11091067
- Yadav, V. K., Gacem, A., Choudhary, N., Rai, A., Kumar, P., Yadav, K. K., et al. (2022a). Status of coal-based thermal power plants, coal fly ash production, utilization in India and their emerging applications. *Minerals* 12, 1503. doi:10.3390/min12121503
- Yadav, V. K., Inwati, G. K., Ali, D., Gnanamoorthy, G., Bera, S. P., Khan, S. H., et al. (2022b). Remediation of azure A dye from aqueous solution by using surface-modified coal fly ash extracted ferrospheres by mineral acids and toxicity assessment. *Adsorpt. Sci. Technol.* 2022, 1–14. doi:10.1155/2022/7012889
- Yadav, V. K., Amari, A., Gacem, A., Elboughdiri, N., Eltayeb, L. B., and Fulekar, M. H. (2023a). Treatment of fly-ash-contaminated wastewater loaded with heavy metals by using fly-ash-synthesized iron oxide nanoparticles. *WaterSwitzerl.* 15, 908. doi:10.3390/w15050908
- Yadav, V. K., Amari, A., Wanale, S. G., Osman, H., and Fulekar, M. H. (2023b). Synthesis of floral-shaped nanosilica from coal fly ash and its application for the remediation of heavy metals from fly ash aqueous solutions. *Sustainability* 15, 2612. doi:10.3390/su15032612
- Yadav, V. (2019). *Nano-based approaches techniques and method development for separation of ferrous alumina and silica from waste fly ash.*

- Yao, Z. T., Xia, M. S., Sarker, P. K., and Chen, T. (2014). A review of the alumina recovery from coal fly ash, with a focus in China. *Fuel* 120, 74–85. doi:10.1016/j.fuel.2013.12.003
- Yoon, S., and Park, I. (2017). Micropore structures in cenosphere-containing cementitious materials using micro-CT. *Adv. Mater. Sci. Eng.* 2017, 1–10. doi:10.1155/2017/3892683
- Yoriya, S., and Tepsri, P. (2020). Separation process and microstructure-chemical composition relationship of cenospheres from lignite fly ash produced from coal-fired power plant in Thailand. *Appl. Sci. Switz.* 10, 5512. doi:10.3390/app10165512
- Yoriya, S., and Tepsri, P. (2021). Crystal growth on cenospheres from high-calcium fly ash. *Cryst. (Basel)* 11. doi:10.3390/cryst11080919
- Yoriya, S., Intana, T., and Tepsri, P. (2019). Separation of cenospheres from lignite fly ash using acetone-water mixture. *Appl. Sci. Switz.* 9, 3792. doi:10.3390/app9183792
- Zhao, Y., Zhang, J., Sun, J., Bai, X., and Zheng, C. (2006). Mineralogy, chemical composition, and microstructure of ferrospheres in fly ashes from coal combustion. *Energy & Fuels* 20, 1490–1497. doi:10.1021/ef060008f
- Zierold, K. M., and Odoh, C. (2020). A review on fly ash from coal-fired power plants: Chemical composition, regulations, and health evidence. *Rev. Environ. Health* 35, 401–418. doi:10.1515/reveh-2019-0039
- Żyrkowski, M., Neto, R. C., Santos, L. F., and Witkowski, K. (2016). Characterization of fly-ash cenospheres from coal-fired power plant unit. *Fuel* 174, 49–53. doi:10.1016/j.fuel.2016.01.061